# Limit cycles in planar piecewise linear systems of saddle-saddle type with a nonregular separation line

Zhouchao Wei[a,b,c], [1] Xiuyuan Cheng[a], Jicheng Duan[a], Irene Moroz[d], Liyun Zhang[e],

[a]School of Mathematics and Physics, China University of Geosciences, Wuhan, 430074, China
[b]Institute for Advanced Marine Research, China University of Geosciences, Guangzhou 511462, China
[c]Shenzhen Research Institute, China University of Geosciences, Shenzhen, 518000, China
[d]Mathematical Institute, University of Oxford, Oxford OX2 6GG, England
[e]Basic Science Department, Wuchang Shouyi University, Wuhan, 430064, China

## Abstract

The maximum number of crossing limit cycles in planar piecewise linear systems with a nonregular separating line is considered. We give the canonical form topological transformation by considering specific assumptions in the planar piecewise linear systems of saddle-saddle type with a nonregular separation line. Based on the classification of the section maps, we analyse the expressions and analytic properties of the composite maps. In particular, some parameter conditions are found that make the systems yield at least five bounded crossing limit cycles.

*Keywords:* Crossing limit cycles; saddle-saddle type; planar piecewise linear systems; nonregular separation line; section maps.

## 1. Introduction

Piecewise smooth systems have been paid more and more attention [1, 9, 13]. Switching boundaries can not only bring more types of invariant sets, e.g. tangent point, crossing limit cycle and sliding limit cycle [20, 27], but also generate chaos in piecewise linear systems [35, 42, 43]. Even low two-dimensional piecewise systems can produce complex behaviors, such as boundary equilibrium bifurcation [18, 22, 38], sliding bifurcation [28, 29], critical crossing cycle bifurcation [15, 44], and pseudo-Hopf bifurcation [5].

Recently, limit cycles have also been an important research topic in planar piecewise linear systems (hereafter PWLSs) [5, 6, 9]. In the last few decades, PWLS have received increasing interest in the modelling of real-world, e.g. biological processes [12], electronic and mechanical devices [4, 39], and control theory [19]. In addition, PWLSs have significant advantages in the design of certain chaotic systems or engineering control systems [30]. The common manifestation of distinct mechanisms for Hopf-like bifurcations is that a stationary solution changes stability or form and small amplitude oscillations are created [40]. Pseudo-Hopf bifurcation,

[1]corresponding author. E-mail address:weizhouchao@163.com(Z. Wei).

also known as the special Hopf-like bifurcations of type I [11], has received some rising attention after the work of [21, 37].

Based on Hilbert's problem in the 16th century and the study of limit cycles in the 19th century with Poincaré, more and more researchers focus on the maximum number of limit cycles in PWLSs. Lum and Chua [36] conjectured that there is at most one limit cycle for a type of continuous PWLS that has only a straight separation line and the vector field is continuous on the separation line, which has been proved in 1998 [14]. However, when sliding bifurcations occur, the dynamic properties of discontinuous PWLS will become more complicated. A general discontinuous piecewise linear systems with two zones was considered that includes all the possible configurations in planar linear systems, and shown the existence of a focus in one zone is sufficient to get three nested limit cycles [16]. The existence of two limit cycles in a class of general planar piecewise linear systems constituted by two linear subsystems with node–node dynamics was proved by the Liénard-like canonical form [24]. A lower bound for the maximum number of nonsliding limit cycles of planar discontinuous piecewise linear differential systems with two zones separated by a straight line was provided, which explanined that the existence of two or three limit cycles in six kinds of planar discontinuous piecewise linear differential systems: F-F, F-N, F-S, N-N, N-S, S-S (we denote focus, saddle, node, center as F, S, N, C, respectively) [7, 17, 23, 32, 33].

When the separation line is no longer straight, PWLSs may generate more limit cycles [8, 34]. In particular, PWLSs are called *linear lateral systems* [45] when the separation line is formed by two rays and the angle between them is not 0 and $\pi$. The linear lateral systems of the C-C type have at most two limit cycles that can be achieved [45]. A class of linear lateral systems of S-C type has been proved to have at most 3 limit cycles [46, 47]. The upper bound of the maximum number of limit cycles for a class of systems with a linear centre is also proved to be sharp [13]. An F-F type linear lateral system can have 5 limit cycles, but this was proved numerically [25]. Refs. [46, 47] proved analytically that a linear lateral system of the F-F type can have at least 5 limit cycles. Liu et al. considered the coexistence of crossing limit cycles and sliding limit cycles by establishing poincaré maps for two subsystems that have same Jacobi matrix [31]. Chen et al. considered the exestence of a unique nonsymmetric limit cycle for a family of three-dimensional PWLSs with three zones separated by two parallel planes [10]. Sun and Du investigated the existence and number of crossing limit cycles in a class of PWLSs with N-N type critical points defined in two zones separated by a nonregular line formed by two rays emanated from the origin, and obtain this class of systems can have two, three or four two-point crossing limit cycles [41]. Based on the first integrals, Baymout et al. considered the maximum number of limit cycles of the discontinuous PWLSs separated by a nonregular line and formed by a linear center and one of the four classes of quadratic centers [3]. By employing the approach of Poincaré maps, Huang and Wang obtained the existence, exact number, and asymptotical stability of periodic solutions are investigated thoroughly in a piecewise smooth system incorporating a new control strategy [26]. Generally, we prefer to find an analytical method that can prove how many limit cycles the system is capable of generating over what range of parameters. As we know, constructing Poincaré maps for the system has always been a commonly used method. However, it is often difficult to determine how many limit cycles the system can generate under a given range of parameters because the maps have

no explicit expressions and have complex convexities. We will consider a kind of linear lateral systems with S-S type, and analytically prove the number of limit cycles under some parameter conditions in this article.

The structure of our article is as follows. Section 2 gives the S-S type linear lateral system we will consider. In sections 3 and 4 we define two Poincaré maps and discuss their properties. In section 5 the results about limit cycles in the PWLSs are obtained. In section 6 we give proofs of the results about the Poincaré maps in section 3 and section 4. A summary is given in section 7.

## 2. Preliminary

Without loss of generality, we assume that one of the rays of the separation line in a linear lateral system is the positive $x$-axis, and that the angle between the two rays is $\alpha$. Denoting

$$\Sigma_\alpha = \begin{cases} \{(x,y): x \geq 0, y = 0\} \cup \{(x,y): y = (\tan\alpha)x, y \geq 0\}, & \alpha \in (0, \frac{\pi}{2}) \cup (\frac{\pi}{2}, \pi), \\ \{(x,y): x \geq 0, y = 0\} \cup \{(x,y): x = 0, y \geq 0\}, & \alpha = \frac{\pi}{2}. \end{cases}$$

The linear lateral system we consider is

$$\dot{\mathbf{x}} = \begin{cases} A^+(\mathbf{x} - \mathbf{x}_e^+), & \mathbf{x} \in \Sigma_\alpha^+, \\ A^-(\mathbf{x} - \mathbf{x}_e^-), & \mathbf{x} \in \Sigma_\alpha^-, \end{cases} \tag{1}$$

where $A^\pm = (a_{ij}^\pm), i, j = 1, 2$ are invertible matrices, $\mathbf{x}_e^\pm = (x_e^\pm, y_e^\pm)^T$ are the equilibrium points. $\Sigma_\alpha^+, \Sigma_\alpha^-$ are the two sector areas of angles $\alpha$ and $2\pi - \alpha$ separated by $\Sigma_\alpha$. Huan and Yang proved that the system (1) is topologically equivalent to a certain lateral system with $\alpha = \frac{\pi}{2}$ [25]. Under the condition $\alpha = \frac{\pi}{2}$, we will study the following system

$$\dot{\mathbf{x}} = \begin{cases} A^+(\mathbf{x} - \mathbf{x}_e^+), & \mathbf{x} \in \Sigma_{\frac{\pi}{2}}^+ \text{ (right system)} \\ A^-(\mathbf{x} - \mathbf{x}_e^-), & \mathbf{x} \in \Sigma_{\frac{\pi}{2}}^- \text{ (left system).} \end{cases} \tag{2}$$

Denote the vector field $(F_1^\pm(\mathbf{x}), F_2^\pm(\mathbf{x}))^T = A^\pm(\mathbf{x} - \mathbf{x}_e^\pm)$, $\mathbf{x}_e^+ = (x_e^+, y_e^+)^T$, and $\mathbf{x}_e^- = (x_e^-, y_e^-)^T$. To distinguish our study from the PWLSs with a straight separation line, we require that the system (2) with S-S type has the possibility to generate limit cycles that cross the positive $x$-axis and the positive $y$-axis simultaneously. Therefore we have to assume:

(A.0) There exists a trajectory connecting positive $x$-axis and positive $y$-axis in left system.

**Lemma 2.1.** If *(A.0)* holds, we have

$$x_e^- < 0, y_e^- < 0. \tag{3}$$

Furthermore, there exists in the left system a trajectory from positive $y$-axis to positive $x$-axis as time increases for $a_{21}^- > 0$ and $a_{12}^- < 0$; there exists in the left system a trajectory from positive $x$-axis to positive $y$-axis as time increases for $a_{21}^- < 0$ and $a_{12}^- > 0$.

**Proof.** We only prove the former because the latter can be obtained similarly. There are two basic properties of trajectories in saddle-type linear systems:
(1) any tangent of any trajectory (except the stable and the unstable manifold) divides the plane into two areas. The equilibrium point $\mathbf{x}_e^-$ and the trajectory will be in different regions;
(2) the angle between any two tangents of any trajectory (except the stable and the unstable manifold) is less than $\pi$. $F_1^-(0,y) = a_{12}^- y - (a_{11}^- x_e^- + a_{12}^- y_e^-)$, $F_2^-(x,0) = a_{21}^- x - (a_{21}^- x_e^- + a_{22}^- y_e^-)$.

If there exists a trajectory from positive $y$-axis to the positive $x$-axis as time increasesin the left system, $F_1^-(0,y)$ will be a decreasing linear function about $y$ (i.e. $a_{12}^- < 0$) and $F_2^-(x,0)$ will be an increasing linear function about $x$ (i.e. $a_{21}^- > 0$). Morover, we can also obtain that $\alpha_1 \in (0, \frac{\pi}{2})$, $\alpha_2 \in (0, \alpha_1)$ and $\mathbf{x}_e^-$ must be in area I ($\mathbf{x}_e^-$ is in the third quadrant, see Figure 1). ■

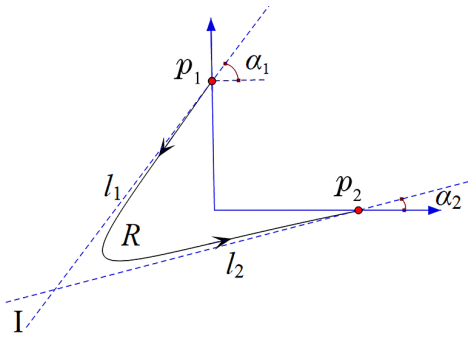


Figure 1: A trajectory connects positive $x$-axis and positive $y$-axis in (2). $l_1$ and $l_2$ are the tangents of trajectory at $p_1$ and $p_2$.

Although we cannot currently rule out the possibility that stable and unstable manifolds of the right system are parallel to the $y$-axis, we assume

$$a_{12}^+ \neq 0. \tag{4}$$

Based on (A.0) and (4), by denoting the eigenvalues of left system and right system as $\lambda_{1,2}^-$ ( $\lambda_1^- < 0 < \lambda_2^-$) and $\lambda_{1,2}^+$ ( $\lambda_1^+ < 0 < \lambda_2^+$), respectively. Remarking $a_{11}^\pm = a^\pm$, $a_{12}^\pm = b^\pm$, $a_{21}^\pm = -(a^\pm - \lambda_1^\pm)(a^\pm - \lambda_2^\pm)/b^\pm$, $a_{22}^\pm = \lambda_1^\pm + \lambda_2^\pm - a^\pm$, we can rewrite $A^\pm$ as

$$A^\pm = \begin{bmatrix} a^\pm & b^\pm \\ -\frac{(a^\pm - \lambda_1^\pm)(a^\pm - \lambda_2^\pm)}{b^\pm} & \lambda_1^\pm + \lambda_2^\pm - a^\pm \end{bmatrix}. \tag{5}$$

Then we can obtain stable manifolds of $x_e^\pm$ ($SM^+$ and $SM^-$)

$$SM^\pm : (\lambda_1^\pm - a^\pm)(x - x_e^\pm) - b^\pm(y - y_e^\pm) = 0, x \neq x_e^\pm,$$

and unstable manifolds ($UM^+$ and $UM^-$)

$$UM^\pm : (\lambda_2^\pm - a^\pm)(x - x_e^\pm) - b^\pm(y - y_e^\pm) = 0, x \neq x_e^\pm.$$

We denote the intersections (if exist) of $SM^{\pm}$ and $x$-axis as $(x_s^{\pm}, 0)$, of $SM^{\pm}$ and $y$-axis as $(0, y_s^{\pm})$, of $UM^{\pm}$ and $x$-axis as $(x_u^{\pm}, 0)$, of $UM^{\pm}$ and $y$-axis as $(0, y_u^{\pm})$, where

$$x_s^{\pm} = \frac{b^{\pm} y_e^{\pm}}{a^{\pm} - \lambda_1^{\pm}} + x_e^{\pm}, \quad y_s^{\pm} = \frac{(a^{\pm} - \lambda_1^{\pm}) x_e^{\pm}}{b^{\pm}} + y_e^{\pm},$$

$$x_u^{\pm} = \frac{b^{\pm} y_e^{\pm}}{a^{\pm} - \lambda_2^{\pm}} + x_e^{\pm}, \quad y_u^{\pm} = \frac{(a^{\pm} - \lambda_2^{\pm}) x_e^{\pm}}{b^{\pm}} + y_e^{\pm}.$$

Note that (A.0) guarantees the existence of $x_s^-, y_s^-, x_u^-, y_u^-$, and (4) guarantees the existence of $y_s^+, y_u^+$. Based on the conditions (A.0) and (4), the system (2) can take many different forms due to the variety of parameters. Here we will only consider some cases so that system (2) can generate more limit cycles. Now we assume that

(A.1) In the left system there is a positive time trajectory from the positive $y$-axis to the origin and then enters the first quadrant;

(A.2) In the right system there is a positive time trajectory that starts from the origin, enters the first quadrant and then arrives at the positive $y$-axis.

**Lemma 2.2.** *(A.1)* guarantees *(A.0)* and is equivalent to the following conditions

$$x_e^- < 0, \quad y_e^- < 0, \quad x_u^- > 0, \quad y_s^- > 0, \quad F_2^-(0,0) \geq 0. \tag{6}$$

*(A.2)* guarantees *(4)* and is equivalent to the following conditions

$$x_e^+ > 0, \quad b^+ < 0, \quad y_t^+ > 0, \quad y_s^+ < 0, \quad F_2^+(0,0) \geq 0, \tag{7}$$

where $(0, y_t^+)$ is the point of tangency between the right system's trajectory and the $y$ axis.

*Proof.* We only give the proof of (7) because (6) is easier to get in a similar way. If (A.2) holds, $F_1^+(0,0) > 0$, $F_1^+(p_2) < 0$, and $F_2^+(0,0) \geq 0$ (see Figure 2). We also can know that $\alpha_1 \in [0, \frac{\pi}{2}), \alpha_2 \in (-\alpha_1, \frac{\pi}{2})$, and $\mathbf{x}_e^+$ will be in the area II. From $F_1^+(0,y) = b^+ y - (a + b^+ k^+) x_e^+$ and $F_1^+(0, y_t^+) = 0$, we have $b^+ < 0$ and $y_t^+ > 0$. In addition, (A.2) means that $SM^+$ cannot intersect the positive $y$-axis and can only intersect the negative $y$-axis (i.e. $y_s^+ < 0$).

In the following, we can first reduce the parameters of the system by topology transformation. Notice that $b^{\pm} < 0$ and $a^- > \lambda_2^- > 0$ (implied by $x_u^- > 0$ in (6)), by transforming

$$\tilde{t} = \begin{cases} \dfrac{a^- b^+}{b^-} t, & \mathbf{x} \in \Sigma_{\frac{\pi}{2}}^+, \\ a^- t, & \mathbf{x} \in \Sigma_{\frac{\pi}{2}}^-, \end{cases} , \tilde{\mathbf{x}} = T\mathbf{x} = \begin{bmatrix} -\dfrac{a^-}{b^-} & 0 \\ 0 & 1 \end{bmatrix} \mathbf{x},$$

we obtain the topologically equivalent form of the system (2)

$$\dot{\tilde{\mathbf{x}}} = \begin{cases} \tilde{A}^+(\tilde{\mathbf{x}} - \tilde{\mathbf{x}}_e^+), & \tilde{\mathbf{x}} \in \Sigma_{\frac{\pi}{2}}^+, \\ \tilde{A}^-(\tilde{\mathbf{x}} - \tilde{\mathbf{x}}_e^-), & \tilde{\mathbf{x}} \in \Sigma_{\frac{\pi}{2}}^-, \end{cases} \tag{8}$$

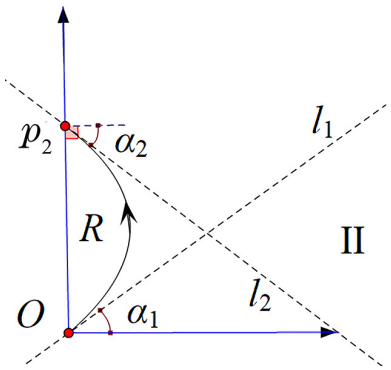


Figure 2: The trajectory $R$ of the right system, which starts from the origin and can arrive at the positive $y$-axis in (2). $l_1$ and $l_2$ are the tangents of $R$ at $O$ and $p_2$ respectively.

where

$$\tilde{A}^+ = \begin{bmatrix} \tilde{a} & -1 \\ (\tilde{a}-\tilde{\lambda}_1^+)(\tilde{a}-\tilde{\lambda}_2^+) & \tilde{\lambda}_1^+ + \tilde{\lambda}_2^+ - \tilde{a} \end{bmatrix}, \tilde{A}^- = \begin{bmatrix} 1 & -1 \\ (1-\tilde{\lambda}_1^-)(1-\tilde{\lambda}_2^-) & \tilde{\lambda}_1^- + \tilde{\lambda}_2^- - 1 \end{bmatrix}, \quad (9)$$

$\tilde{\lambda}_1^\pm$ and $\tilde{\lambda}_2^\pm$ are eigenvalues of $\tilde{A}^\pm$. The algebraic relationship of the parameters in (5) and (9) is given:

$$\tilde{a} = \frac{b^-}{a^- b^+} a^+, \quad \tilde{\lambda}_1^+ = \frac{b^-}{a^- b^+}\lambda_1^+, \quad \tilde{\lambda}_2^+ = \frac{b^-}{a^- b^+}\lambda_2^+, \tilde{\lambda}_1^- = \frac{1}{a^-}\lambda_1^-, \quad \tilde{\lambda}_2^- = \frac{1}{a^-}\lambda_2^-.$$

The relationship between the equilibrium points in (5) and (9) is also given:

$$\tilde{\mathbf{x}}_e^+ = T\mathbf{x}_e^+, \quad \tilde{\mathbf{x}}_e^- = T\mathbf{x}_e^-.$$

**Theorem 2.3.** Under the assumption *(A.1)* and *(A.2)*, the system *(2)* of type S-S is topologically equivalent to the system *(8)*.

To better consider the system (8), we set $a^- = 1, b^- = -1, b^+ = -1$ in (5) (without losing generality). Denoting

$$k^\pm = \frac{y_e^\pm}{x_e^\pm},$$

and the point of tangency between the trajectories of left system and $y$-axis as $(0, y_t^-)$. Combined with the Lemma 2.2, we can easily obtain

$$y_t^+ = -(a-k^+)x_e^+, \quad y_t^- = -(1-k^-)x_e^-. \quad (10)$$

Based on (2), (5), (6) and (7), we will study the following system

$$\dot{\mathbf{x}} = \begin{cases} B^+(\mathbf{x}-\mathbf{x}_e^+), & \mathbf{x} \in \Sigma_{\frac{\pi}{2}}^+, \\ B^-(\mathbf{x}-\mathbf{x}_e^-), & \mathbf{x} \in \Sigma_{\frac{\pi}{2}}^-, \end{cases} \quad (11)$$

where

$$B^+ = \begin{bmatrix} a & -1 \\ (a-\lambda_1^+)(a-\lambda_2^+) & \lambda_1^+ + \lambda_2^+ - a \end{bmatrix}, B^- = \begin{bmatrix} 1 & -1 \\ (1-\lambda_1^-)(1-\lambda_2^-) & \lambda_1^- + \lambda_2^- - 1 \end{bmatrix},$$

and corresponding ranges of the nine parameters for system (11) should satisfy

$$\begin{aligned} & 0 < 1-\lambda_2^- < k^- \le \frac{\lambda_1^-\lambda_2^-}{1-\lambda_1^- - \lambda_2^-} + 1, \quad x_e^- < 0 \\ & x_e^+ > 0, \begin{cases} a < k^+ < a - \lambda_1^+, & \text{if } a \ge \lambda_1^+ \\ a < k^+ \le \frac{\lambda_1^+\lambda_2^+}{a-\lambda_1^+-\lambda_2^+} + a, & \text{if } a < \lambda_1^+ \end{cases} \end{aligned} \tag{12}$$

Now we will give definitions of section maps in the right and left systems of (11) and then discuss their properties. All discussions will be based on conditions (12).

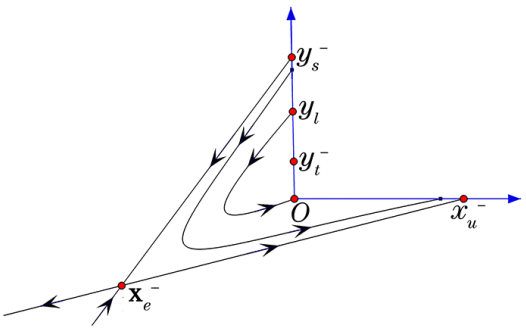


Figure 3: Phase portrait sketch of left system in (11).

## 3. The left section map $\tilde{S}^-$

The phase portrait of left system has the characteristics that $\mathbf{x}_e^-$ is in the third quadrant, $UM^-$ intersects the positive $x$-axis and $SM^-$ intersects the positive $y$-axis. The boundary of the corresponding trajectory of $\tilde{S}^-$ is marked by $UM^-$ and $SM^-$, see Figure 3. The solution $\mathbf{\Phi}^-(t,P)$ of left system (see Figure 3) that starts from point $P(x,y)$ in (11) will be the following form:

$$\begin{aligned} \mathbf{\Phi}^-(t,P) &= \left(\phi_1^-, \phi_2^-\right) \\ &= \frac{1}{\lambda_2^- - \lambda_1^-} \begin{bmatrix} \left(1-\lambda_1^-\right)e^{\lambda_2 t} - \left(1-\lambda_2^-\right)e^{\lambda_1^- t} & e^{\lambda_1^- t} - e^{\lambda_2 t} \\ \left(1-\lambda_1^-\right)\left(1-\lambda_2^-\right)\left(e^{\lambda_2^- t} - e^{\lambda_1^- t}\right) & \left(1-\lambda_1^-\right)e^{\lambda_1^- t} - \left(1-\lambda_2^-\right)e^{\lambda_2^- t} \end{bmatrix} \\ &\quad \cdot \begin{bmatrix} x - x_e^- \\ y - k^- x_e^- \end{bmatrix} + \begin{bmatrix} x_e^- \\ k^- x_e^- \end{bmatrix} \end{aligned} \tag{13}$$

Denoting

$$\Gamma = \{(x, y) : x = 0, y \geq 0\}, \quad \chi = \{(x, y) : x \geq 0, y = 0\},$$

we can define the left section map $\tilde{S}_1^-$.

**Definition 3.1.** Let the map $\tilde{S}_1^- : P_1 \mapsto P_2$, if for a point $P_1 \in \Gamma$, there exists a $t > 0$ and a point $P_2 \in \Sigma_{\frac{\pi}{2}}$ such that $\mathbf{\Phi}^-(t, P_1) = P_2$.

**Remark 3.1.** The $t$ in the Definition 3.1 is unique if it exists, because trajectories of a saddle-type system can pass through a straight line at most twice, so our definition is well defined.

We divide $\tilde{S}_1^-$ into two parts

$$\begin{aligned} \tilde{S}_1^- &: (0, y_0^-) \mapsto (0, y_1^-), \quad y_1^- \geq 0, \\ \tilde{S}_2^- &: (0, y_0^-) \mapsto (x_1^-, 0), \quad x_1^- \geq 0, \end{aligned}$$

and take $S_1^- : y_0^- \mapsto y_1^-$ and $S_2^- : y_0^- \mapsto x_1^-$ for the convenience of discussions.

**Theorem 3.1.** Denoting $y_l = \phi_2^-(-t_l, (0, 0))$ (see Figure 3). The value of $t_l$ can be obtained from the only positive zero point of the following function

$$h_l(t) = (1 - \lambda_1^- - k^-)e^{-\lambda_2 t} - (1 - \lambda_2^- - k^-)e^{-\lambda_1 t} - (\lambda_2^- - \lambda_1^-).$$

We have $S_1^- : (y_t^-, y_l] \to [0, y_t^-), y_0^- \mapsto y_1^-$, which satisfies

$$\begin{cases} y_0^-(t) = x_e^-[k^- - 1 - \dfrac{\lambda_2^- e^{\lambda_1^- t} - \lambda_1^- e^{\lambda_2^- t} - (\lambda_2^- - \lambda_1^-)}{e^{\lambda_2^- t} - e^{\lambda_1^- t}}], \\ y_1^-(t) = x_e^-[k^- - 1 + \dfrac{\lambda_2^- e^{\lambda_2^- t} - \lambda_1^- e^{\lambda_1^- t} - (\lambda_2^- - \lambda_1^-)e^{(\lambda_1^- + \lambda_2^-)t}}{e^{\lambda_2^- t} - e^{\lambda_1^- t}}], \end{cases} \quad t \in (0, t_l], \tag{14}$$

and $S_2^- : (y_l, y_s^-) \to (0, x_u^-), y_0^- \mapsto x_1^-$, which satisfies

$$\begin{cases} y_0^-(t) = x_e^-[k^- - \dfrac{(1 - \lambda_1^-)(1 - \lambda_2^-)(e^{\lambda_2^- t} - e^{\lambda_1^- t}) - (\lambda_2^- - \lambda_1^-)k^-}{(1 - \lambda_2^-)e^{\lambda_2^- t} - (1 - \lambda_1^-)e^{\lambda_1^- t}}], \\ x_1^-(t) = x_e^-[1 - \dfrac{(e^{\lambda_2^- t} - e^{\lambda_1^- t})k^- - (\lambda_2^- - \lambda_1^-)e^{(\lambda_1^- + \lambda_2^-)t}}{(1 - \lambda_2^-)e^{\lambda_2^- t} - (1 - \lambda_1^-)e^{\lambda_1^- t}}], \end{cases} \quad t \in (t_l, +\infty). \tag{15}$$

In addition, we have following results about $S_1^-$:

(a1) $\lim\limits_{t \to 0} y_0^-(t) = \lim\limits_{t \to 0} y_1^-(t) = y_t^-$, $y_0^-(t_l) = y_l$ and $y_1^-(t_l) = 0$;

(b1) $y_0^-(t)$ monotonically increases and $y_1^-(t)$ decreases as $t$ increases. $y_0^-$ monotonically decreases as $y_1^-$ increases;

(c1) $\lim\limits_{t \to 0} \dfrac{\mathrm{d}y_0^-(t)}{\mathrm{d}y_1^-(t)} = \lim\limits_{y_1^- \to y_t^-} \dfrac{\mathrm{d}y_0^-}{\mathrm{d}y_1^-} = -1$;

(d1) $\dfrac{\mathrm{d}^2 y_0^-}{\mathrm{d}{y_1^-}^2}$ is $\begin{cases} \text{positive}, & \lambda_1^- + \lambda_2^- < 0, \\ 0, & \lambda_1^- + \lambda_2^- = 0, \\ \text{negative}, & \lambda_1^- + \lambda_2^- > 0. \end{cases}$

We have following results about $S_2^-$:

(a2) $\lim\limits_{t\to t_l} y_0^-(t) = y_l$, $\lim\limits_{t\to t_l} x_1^-(t) = 0$, $\lim\limits_{t\to+\infty} y_0^-(t) = y_s^-$ and $\lim\limits_{t\to+\infty} x_1^-(t) = x_u^-$;

(b2) $y_0^-(t)$ and $x_1^-(t)$ both monotonically increase as $t$ increases. $y_0^-$ monotonically increases as $x_1^-$ increases;

(c2) $\lim\limits_{t\to+\infty} \dfrac{\mathrm{d}y_0^-(t)}{\mathrm{d}x_1^-(t)} = \lim\limits_{x_1^-\to x_u^-} \dfrac{\mathrm{d}y_0^-}{\mathrm{d}x_1^-} = \begin{cases} 0, & \lambda_1^- + \lambda_2^- > 0, \\ k^-, & \lambda_1^- + \lambda_2^- = 0, \\ +\infty, & \lambda_1^- + \lambda_2^- < 0. \end{cases}$

Moreover, if $k^- = \frac{\lambda_1^-\lambda_2^-}{1-\lambda_1^--\lambda_2^-} + 1$, $\lim\limits_{t\to t_l} \dfrac{\mathrm{d}y_0^-(t)}{\mathrm{d}x_1^-(t)} = \lim\limits_{x_1^-\to 0} \dfrac{\mathrm{d}y_0^-}{\mathrm{d}x_1^-} = 0$;

(d2-A) If $\lambda_1^- + \lambda_2^- \le 0$, $\dfrac{\mathrm{d}^2 y_0^-}{\mathrm{d}{x_1^-}^2} > 0$;

(d2-B) If $\lambda_1^- + \lambda_2^- > 0$, there exists a decreasing inflection function

$$K_l(t) = \frac{-(\lambda_1^- + \lambda_2^-)m_l(t) + \sqrt{(\lambda_1^- + \lambda_2^-)^2 m_l^2(t) + 4(\lambda_2^- - \lambda_1^-)^2(1-\lambda_1^-)(1-\lambda_2^-)e^{(\lambda_1^-+\lambda_2^-)t}}}{2(\lambda_2^- - \lambda_1^-)}, t \in (t_l, +\infty), \tag{16}$$

where $m_l(t) = (1-\lambda_2^-)e^{\lambda_2^- t} - (1-\lambda_1^-)e^{\lambda_1^- t}$. Moreover, for $t \in (t_l, +\infty)$, $0 < K_l(t) < K_l(t_l)$. Denote $\Delta_l(k^-) \triangleq K_l(t_l(k^-)) - k^-$, then one of the following assertions *(d2-B1)* and *(d2-B2)* must hold:

(d2-B1) If $\Delta_l(k^-) \le 0$, then $\dfrac{\mathrm{d}^2 y_0^-}{\mathrm{d}{x_1^-}^2} < 0$;

(d2-B2) If $\Delta_l(k^-) > 0$, there exists a $t_0^- = K_l^{-1}(k^-)$ such that $\dfrac{\mathrm{d}^2 y_0^-(t)}{\mathrm{d}{x_1^-}^2(t)}$ is $\begin{cases} \text{positive}, & t_l < t < t_0^-, \\ 0, & t = t_0^-, \\ \text{negative}, & t > t_0^-, \end{cases}$

where $t_l(k^-)$ is the inverse function determined by

$$k^- = 1 - \frac{\lambda_2^- e^{-\lambda_1^- t_l} - \lambda_1^- e^{-\lambda_2^- t_l} - (\lambda_2^- - \lambda_1^-)}{e^{-\lambda_1^- t_l} - e^{-\lambda_2^- t_l}}; \tag{17}$$

(d2-C) If $\lambda_1^- + \lambda_2^- > 0$, then $\lim\limits_{k^-\to 1-\lambda_2^-} \Delta_l(k^-) < 0$, and $\Delta_l(k^-)\big|_{k^- = \frac{\lambda_1^-\lambda_2^-}{1-\lambda_1^--\lambda_2^-}+1} > 0$. ■

Here we do not prove Theorem 3.1 but give the proof in section 6.

## 4. The right section map $\tilde{S}^+$

If we denote the solution of the right-hand system starting at point $P(x, y)$ as $\mathbf{\Phi}^+(t, P)$, we similarly obtain

$$\begin{aligned}\mathbf{\Phi}^+(t,P) &= \left(\phi_1^+, \phi_2^+\right) \\ &= \frac{1}{\lambda_2^+ - \lambda_1^+} \begin{bmatrix} \left(a-\lambda_1^+\right) e^{\lambda_2^+ t} - \left(a-\lambda_2^+\right) e^{\lambda_1^+ t} & e^{\lambda_1^+ t} - e^{\lambda_2^+ t} \\ \left(a-\lambda_1^+\right)\left(a-\lambda_2^+\right)\left(e^{\lambda_2^+ t} - e^{\lambda_1^+ t}\right) & \left(a-\lambda_1^+\right) e^{\lambda_1^+ t} - \left(a-\lambda_2^+\right) e^{\lambda_2^+ t} \end{bmatrix} \\ &\quad \cdot \begin{bmatrix} x - x_e^+ \\ y - k^+ x_e^+ \end{bmatrix} + \begin{bmatrix} x_e^+ \\ k^+ x_e^+ \end{bmatrix}\end{aligned} \tag{18}$$

Next we give the definition of the right section map $\tilde{S}^+$.

**Definition 4.1.** Let the map $\tilde{S}^+ : Q_1 \mapsto Q_2$, if for a point $Q_1 \in \Sigma_{\frac{\pi}{2}}$, there exists a $t > 0$ and a point $Q_2 \in \Gamma$ such that $\mathbf{\Phi}^+(t, Q_1) = Q_2$.

**Remark 4.1.** In a similar way to the remark 3.1, we know that this definition is also well defined.

We will present our results according to the corresponding types of phase portraits of the right system, since the situation of the right section map is more complicated than the left one. Before doing so, we will divide $\tilde{S}^+$ into two parts

$$\begin{aligned}\tilde{S}_1^+ &: (0, y_1^+) \mapsto (0, y_0^+), \quad y_1^+ \geq 0, \\ \tilde{S}_2^+ &: (x_1^+, 0) \mapsto (0, y_0^+), \quad x_1^+ \geq 0,\end{aligned}$$

and take $S_1^+ : y_1^+ \mapsto y_0^+$, $S_2^+ : x_1^+ \mapsto y_0^+$ for the convenience of discussion. Then by denoting $y_r = \phi_2^+(t_r, (0,0))$, where $t_r$ is the unique positive zero point of function

$$h_r(t) = (a - \lambda_1^+ - k^+)e^{\lambda_2^+ t} - (a - \lambda_2^+ - k^+)e^{\lambda_1^+ t} - (\lambda_2^+ - \lambda_1^+),$$

which will be given in section 6.

Now we will classify and discuss the position of the equilibrium point $\mathbf{x}_e^+$. The boundary of the corresponding trajectory of $S^+$ is marked by $SM^+$ and $UM^+$. If $\mathbf{x}_e^+$ is in the first quadrant, $k^+ > 0$ and the slope of the line represented by $SM^+$ is positive (see Figure 4). If $\mathbf{x}_e^+$ is on the positive $x$-axis, then $k = 0$ and $SM^+$ has a positive slope, see Figure 5.

**Theorem 4.1.** For arbitrary $k^+$, we have $S_1^+ : [0, y_t^+) \to (y_t^+, y_r], y_1^+ \mapsto y_0^+$, which satisfies

$$\begin{cases} y_0^+(t) = x_e^+[k^+ - a + \dfrac{\lambda_2^+ e^{-\lambda_1^+ t} - \lambda_1 e^{-\lambda_2^+ t} - (\lambda_2^+ - \lambda_1^+)}{e^{-\lambda_1^+ t} - e^{-\lambda_2^+ t}}], \\ y_1^+(t) = x_e^+[k^+ - a - \dfrac{\lambda_2^+ e^{-\lambda_2^+ t} - \lambda_1^+ e^{-\lambda_1^+ t} - (\lambda_2^+ - \lambda_1^+)e^{-(\lambda_1^+ + \lambda_2^+)t}}{e^{-\lambda_1^+ t} - e^{-\lambda_2^+ t}}], \end{cases} \quad t \in (0, t_r]. \tag{19}$$

In addition,we have following results about $S_1^+$:

(a1) $\lim\limits_{t\to 0} y_0^+(t) = \lim\limits_{t\to 0} y_1^+(t) = y_t^+$, $y_0^+(t_r) = y_r$ and $y_1^+(t_r) = 0$;

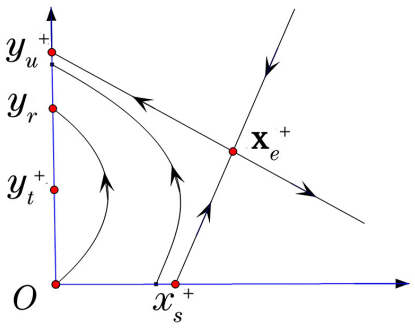


Figure 4: Phase portrait sketch of right system when $k^+ > 0$ in (11).

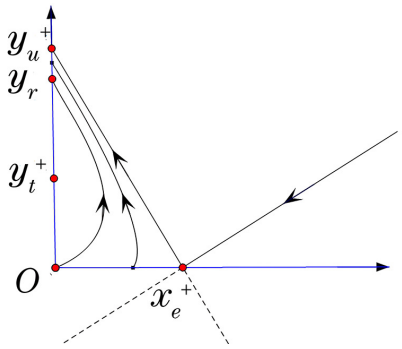


Figure 5: Phase portrait sketch of right system when $k^+ = 0$ in (11).

(b1) $y_0^+(t)$ monotonically increases and $y_1^+(t)$ decreases as $t$ increases. $y_0^+$ monotonically decreases as $y_1^+$ increases;

(c1) $\lim\limits_{t\to 0}\dfrac{\mathrm{d}y_0^+(t)}{\mathrm{d}y_1^+(t)} = \lim\limits_{y_1^+\to y_t^+}\dfrac{\mathrm{d}y_0^+}{\mathrm{d}y_1^+} = -1$;

(d1) $\dfrac{\mathrm{d}^2 y_0^+}{\mathrm{d}{y_1^+}^2}$ is $\begin{cases}\text{positive}, & \lambda_1^+ + \lambda_2^+ < 0,\\ 0, & \lambda_1^+ + \lambda_2^+ = 0,\\ \text{negative}, & \lambda_1^+ + \lambda_2^+ > 0.\end{cases}$

Here we need to emphasise that $S_2^+$ is more complex than $S_1^+$, so we need to discuss the results about $S_2^+$ based on the ranges of the parameters $k^+$ and $\lambda_1^+$.

**Theorem 4.2.** If $k^+ > 0$ (see Figure 4), we have $S_2^+ : (0, x_s^+) \to (y_r, y_u^+), x_1^+ \mapsto y_0^+$, which satisfies

$$\begin{cases} y_0^+(t) = x_e^+[k^+ + \dfrac{(a-\lambda_1^+)(a-\lambda_2^-)(e^{-\lambda_2^+ t} - e^{-\lambda_1^+ t}) - (\lambda_2^+ - \lambda_1^+)k^+}{(a-\lambda_1^+)e^{-\lambda_1^+ t} - (a-\lambda_2^+)e^{-\lambda_2^+ t}}], \\ x_1^+(t) = x_e^+[1 + \dfrac{(e^{-\lambda_2^+ t} - e^{-\lambda_1^+ t})k^+ - (\lambda_2^+ - \lambda_1^+)e^{-(\lambda_1^+ + \lambda_2^+)t}}{(a-\lambda_1^+)e^{-\lambda_1^+ t} - (a-\lambda_2^+)e^{-\lambda_2^+ t}}], \end{cases} \quad t \in (t_r, +\infty). \tag{20}$$

We have following results about $S_2^+$:

(a2) $\lim\limits_{t\to t_r} y_0^+(t) = y_r$, $\lim\limits_{t\to t_r} x_1^+(t) = 0$, $\lim\limits_{t\to+\infty} y_0^+(t) = y_u^+$ and $\lim\limits_{t\to+\infty} x_1^+(t) = x_s^+$;

(b2) $y_0^+(t)$ and $x_1^+(t)$ monotonically increase as $t$ increases. $y_0^+$ monotonically increases as $x_1^+$ increases;

(c2) $\lim\limits_{t\to+\infty}\dfrac{\mathrm{d}y_0^+(t)}{\mathrm{d}x_1^+(t)} = \lim\limits_{x_1^+\to x_s^+}\dfrac{\mathrm{d}y_0^+}{\mathrm{d}x_1^+} = \begin{cases}+\infty, & \lambda_1^+ + \lambda_2^+ > 0,\\ k^+, & \lambda_1^+ + \lambda_2^+ = 0,\\ 0, & \lambda_1^+ + \lambda_2^+ < 0.\end{cases}$

**Theorem 4.3.** If $k^+ = 0$ (see Figure 5), we have $S_2^+ : (0, x_e^+) \to (y_r, y_u^+), x_1^+ \mapsto y_0^+$, which satisfies the same parametric equations as *(20)*.

In addition, about $S_2^+$ we have following results:

(a) $\lim\limits_{t\to t_r} y_0^+(t) = y_r$, $\lim\limits_{t\to t_r} x_1^+(t) = 0$, $\lim\limits_{t\to+\infty} y_0^+(t) = y_u^+$ and $\lim\limits_{t\to+\infty} x_1^+(t) = x_e^+$;

(b) The same as (b2) in Theorem 4.2;

(c) $\lim\limits_{t\to+\infty} \dfrac{\mathrm{d}y_0^+(t)}{\mathrm{d}x_1^+(t)} = \lim\limits_{x_1^+\to x_e^+} \dfrac{\mathrm{d}y_0^+}{\mathrm{d}x_1^+} = 0.$

**Theorem 4.4.** If $k^+ < 0$ and $a > \lambda_1^+$ (see Figure 6), by denoting from $F_2^+(x_t^+, 0) = 0$

$$x_t^+ = x_e^+[1 + \frac{k^+(\lambda_1^+ + \lambda_2^+ - a)}{(a-\lambda_1^+)(a-\lambda_2^+)}],$$

we have $S_2^+ : (0, x_t^+] \to (y_r, \phi_2^+(t_{g_r}^0, (x_t^+, 0))], x_1^+ \mapsto y_0^+$, which satisfies the same parametric equations as *(20)* but $t \in (t_r, t_{g_r}^0]$, where $t_{g_r}^0$ is the only zero point of function

$$g_r(t) = k^+[\lambda_2(a-\lambda_2^+)e^{\lambda_1^+ t} - \lambda_1^+(a-\lambda_1^+)e^{\lambda_2^+ t}] - (\lambda_2^+ - \lambda_1^+)(a-\lambda_1^+)(a-\lambda_2^+).$$

In addition, about $S_2^+$ we have following results:

(a) $y_0^+(t_r) = y_r$, $x_1^+(t_r) = 0$, $y_0^+(t_{g_r}^0) = \phi_2^+(t_{g_r}^0, (x_t^+, 0))$ and $x_1^+(t_{g_r}^0) = x_t^+$;

(b) The same as (b2) in Theorem 4.2;

(c) $\dfrac{\mathrm{d}y_0^+(t)}{\mathrm{d}x_1^+(t)}|_{t=t_{g_r}^0} = \dfrac{\mathrm{d}y_0^+}{\mathrm{d}x_1^+}|_{x_1^+=x_t^+} = 0.$

The phase portrait of the right system in this case has the characteristics that $\mathbf{x}_e^+$ is in the fourth quadrant and $SM^+$ has a positive slope. The corresponding trajectory tangent to the $x$-axis at $(x_t^+, 0)$, see Figure 6.

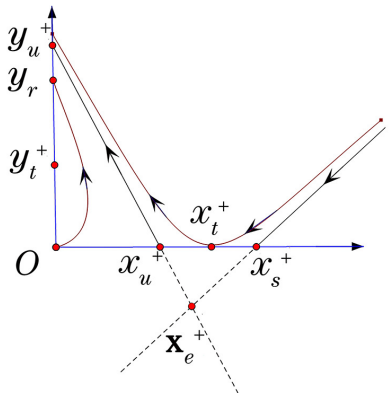


Figure 6: Phase portrait sketch of right system when $k^+ < 0$ and $a > \lambda_1^+$ in (11).

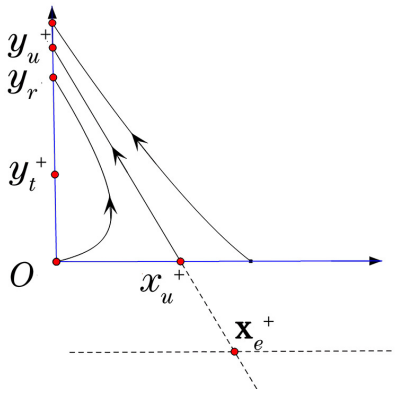


Figure 7: Phase portrait sketch of right system when $a = \lambda_1^+$ in (11).

**Theorem 4.5.** If $a = \lambda_1^+$ (which implies $k^+ < 0$, see Figure 7) , we have $S_2^+ : [0, +\infty) \to [y_r, +\infty), x_1^+ \mapsto y_0^+$, which satisfies the same parametric equations as *(20)*. In addition, we have the following results about $S_2^+$:

(a) $\lim\limits_{t\to t_r} y_0^+(t) = y_r$, $\lim\limits_{t\to t_r} x_1^+(t) = 0$, $\lim\limits_{t\to+\infty} y_0^+(t) = +\infty$ and $\lim\limits_{t\to+\infty} x_1^+(t) = +\infty$;

(b) The same as (b2) in Theorem 4.2;

(c) $\lim\limits_{t\to+\infty}\dfrac{\mathrm{d}y_0^+(t)}{\mathrm{d}x_1^+(t)}=\lim\limits_{x_1^+\to+\infty}\dfrac{\mathrm{d}y_0^+}{\mathrm{d}x_1^+}=0.$

The phase portrait of the right system in this case has the characteristics that $\mathbf{x}_e^+$ is in the fourth quadrant and the slope of $SM^+$ is 0. The corresponding trajectories of $S^+$ extend to infinity, see Figure 7. Finally, the most important theorem will be the main basis for our conclusions about limit cycles.

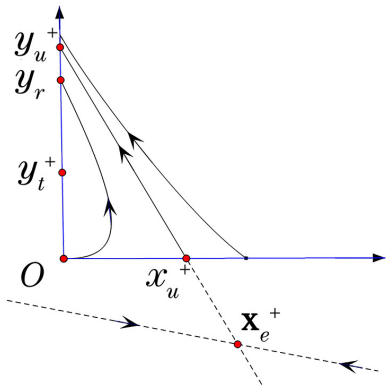


Figure 8: Phase portrait sketch of right system when $a<\lambda_1^+$ in (11).

**Theorem 4.6.** If $a<\lambda_1^+$ (which implies $k^+<0$, see Figure 8), we denote

$$p(a)=-[\frac{(\lambda_1^+-a)^{\lambda_2^+}}{(\lambda_2^+-a)^{\lambda_1^+}}]^{\frac{1}{\lambda_2^+-\lambda_1^+}}, \tag{21}$$

$$k_p=[\frac{(\lambda_2^+-a)^{\lambda_2^+}}{(\lambda_1^+-a)^{\lambda_1^+}}]^{\frac{1}{\lambda_2^+-\lambda_1^+}}, \tag{22}$$

$$b_p=x_e^+[(\lambda_2^+-a)^{\frac{-\lambda_1^+}{\lambda_2^+-\lambda_1^+}}-(\lambda_1^+-a)^{\frac{-\lambda_1^+}{\lambda_2^+-\lambda_1^+}}][(\lambda_2^+-a)^{\frac{\lambda_2^+}{\lambda_2^+-\lambda_1^+}}-(\lambda_1^+-a)^{\frac{\lambda_2^+}{\lambda_2^+-\lambda_1^+}}]. \tag{23}$$

Meanwhile, we denote $t_{m_r}^0$ as the unique zero point of function

$$m_r(t)=(a-\lambda_1^+)e^{-\lambda_1^+t}-(a-\lambda_2^+)e^{-\lambda_2^+t}.$$

Then we will consider three cases according to the value of $k^+$:

Case 1: $a<k^+<p(a)$

We have $S_2^+:(0,+\infty)\to(y_r,+\infty),x_1^+\mapsto y_0^+$, which satisfies the same parametric equations as *(20)* but $t\in(t_r,t_{m_r}^0)$. In addition, about $S_2^+$ following results hold:

(a1) $\lim\limits_{t\to t_r}y_0^+(t)=y_r$, $\lim\limits_{t\to t_r}x_1^+(t)=0$, $\lim\limits_{t\to t_{mr}^0}y_0^+(t)=+\infty$ and $\lim\limits_{t\to t_{mr}^0}x_1^+(t)=+\infty$;

(b1) $y_0^+(t)$ and $x_1^+(t)$ monotonically increase as $t$ increases. $y_0^+$ monotonically increases as $x_1^+$ increases;

(c1) The graph of map $S_2^+$ has the asymptote $y_0^+ = k_p x_1^+ + b_p$,

(d1-A) If $\lambda_1^+ + \lambda_2^+ \geq 0$, $\dfrac{\mathrm{d}^2 y_0^+}{\mathrm{d}{x_1^+}^2} < 0$;

(d1-B) If $\lambda_1^+ + \lambda_2^+ < 0$, there exists an increasing inflection function

$$K_r(t) = \frac{(\lambda_1^+ + \lambda_2^+)m_r(t) - \sqrt{(\lambda_1^+ + \lambda_2^+)^2 m_r^2(t) + 4(\lambda_2^+ - \lambda_1^+)^2(a - \lambda_1^+)(a - \lambda_2^+)e^{-(\lambda_1^+ + \lambda_2^+)t}}}{2(\lambda_2^+ - \lambda_1^+)}, t \in (t_r, t_{m_r}^0). \tag{24}$$

Moreover, for $t \in (t_r, t_{m_r}^0)$, $K_r(t_r) < K_r(t) < p(a)$. Denote $\Delta_r(k^+) \triangleq K_r(t_r(k^+)) - k^+$, then one of the following assertions (d1-B1) and (d1-B2) must hold:

(d1-B1) If $\Delta_r(k^+) \geq 0$, then $\dfrac{\mathrm{d}^2 y_0^+}{\mathrm{d}{x_1^+}^2} < 0$;

(d1-B2) If $\Delta_r(k^+) < 0$, there exists a $t_0^+ = K_r^{-1}(k^+)$ such that $\dfrac{\mathrm{d}^2 y_0^+}{\mathrm{d}{x_1^+}^2}$ is $\begin{cases} \text{positive}, & t_r < t < t_0^+, \\ 0, & t = t_0^+, \\ \text{negative}, & t_0^+ < t < t_{m_r}^0, \end{cases}$

where the $t_r(k^+)$ is the inverse function determined by

$$k^+ = a + \frac{\lambda_2^+ e^{\lambda_1^+ t_r} - \lambda_1^+ e^{\lambda_2^+ t_r} - (\lambda_2^+ - \lambda_1^+)}{e^{\lambda_2^+ t_r} - e^{\lambda_1^+ t_r}}. \tag{25}$$

In particular, if $\lambda_1^+ + \lambda_2^+ < 0$, then $\lim\limits_{k^+ \to p(a)} \Delta_r(k^+) > 0$.

Case 2: $p(a) < k^+ \leq \dfrac{\lambda_1^+ \lambda_2^+}{a - \lambda_1^+ - \lambda_2^+} + a$

We have $S_2^+ : (0, +\infty) \to (y_r, +\infty), x_1^+ \mapsto y_0^+$, which satisfies the same parametric equations as *(20)* but $t \in (t_{m_r}^0, t_r)$. In addition, about $S_2^+$ following results hold:

(a2) The same as (a1) in Theorem 4.6;

(b2) $y_0^+(t)$ and $x_1^+(t)$ monotonically decrease as $t$ increases. $y_0^+$ monotonically increases as $x_1^+$ increases;

(c2) The same as (c1) in Theorem 4.6;

(d2-A) If $\lambda_1^+ + \lambda_2^+ \leq 0$, $\dfrac{\mathrm{d}^2 y_0^+}{\mathrm{d}{x_1^+}^2} > 0$;

(d2-B) If $\lambda_1^+ + \lambda_2^+ > 0$, the inflection function $K_r(t)$ is still increasing but $t \in (t_{m_r}^0, t_r)$. Moreover, for $t \in (t_{m_r}^0, t_r)$, $p(a) < K_r(t) < K_r(t_r)$. Furthermore one of the following assertions (d2-B1) and (d2-B2) must hold:

(d2-B1) If $\Delta_r(k^+) \leq 0$, then $\dfrac{\mathrm{d}^2 y_0^+}{\mathrm{d}{x_1^+}^2} > 0$;

(d2-B2) If $\Delta_r(k^+) > 0$, there exists a $t_0^+ = K_r^{-1}(k^+)$ such that $\dfrac{\mathrm{d}^2 y_0^+}{\mathrm{d}{x_1^+}^2}$ is $\begin{cases} \text{positive}, & t_{m_r}^0 < t < t_0^+, \\ 0, & t = t_0^+, \\ \text{negative}, & t_0^+ < t < t_r, \end{cases}$

In particular, if $\lambda_1^+ + \lambda_2^+ > 0$, then $\lim\limits_{k^+ \to p(a)} \Delta_r(k^+) < 0$ and $\Delta_r(k^+)|_{k^+ = \frac{\lambda_1^+\lambda_2^+}{a-\lambda_1^+-\lambda_2^+}+a} = 0$.

Case 3: $k^+ = p(a)$

We have $S_2^+ : (0, +\infty) \to (y_r, +\infty), x_1^+ \mapsto y_0^+$, which has the expression $y_0^+ = k_p x_1^+ + b_p$. For every $x_1^+ \in (0, +\infty)$, it holds that

$$\mathbf{\Phi}^+(t_{m_r}^0, (x_1^+, 0)) = (0, y_0^+), \quad t_{m_r}^0 = t_{g_r}^0 = t_r.$$

Besides, $y_r = b_p$. If $\lambda_1^+ + \lambda_2^+ = 0$, we have $b_p = 2y_t^+ = -2x_e^+(a + \sqrt{a^2 - \lambda_2^{+2}})$ and $k_p = \sqrt{a^2 - \lambda_2^{+2}}$. ■

The phase portrait of the right system in this case has the characteristics that $\mathbf{x}_e^+$ is in the fourth quadrant and $SM^+$ has a negative slope. The corresponding trajectories of $S^+$ extend to infinity but take finite time from $(x_1^+, 0)$ to $(0, y_0^+)$, see Figure 8.

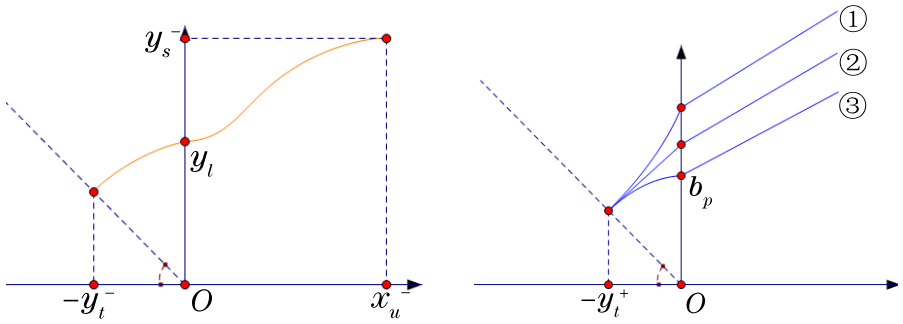


(a) $f^-$ when $k^- = \frac{\lambda_1^-\lambda_2^-}{1-\lambda_1^--\lambda_2^-} + 1$ and $\lambda_1^- + \lambda_2^- > 0$

(b) $f^+$ when $k^+ = p(a)$ and ①$\lambda_1^+ + \lambda_2^+ < 0$, ②$\lambda_1^+ + \lambda_2^+ = 0$, ③$\lambda_1^+ + \lambda_2^+ > 0$

Figure 9: The graph sketchs of $f^-$ and $f^+$

## 5. Crossing limit cycles in the system (11)

First, we introduce a way to draw the two parts of each $S^\pm$ in a Cartesian coordinate system. For $S_1^-$ ($S_1^+$) we define $f^-(-y_1^-) = y_0^-$ ($f^+(-y_1^+) = y_0^+$). For $S_2^-$ ($S_2^+$) we define $f^-(x_1^-) = y_0^-$ ($f^+(x_1^+) = y_0^+$). The functions obtained in this way (see Figure 9) are denoted $f^-$ (orange) and $f^+$ (blue). Then, for convenience, we denote $f_1^\pm = f^\pm|_{x<0}$ and $f_2^\pm = f^\pm|_{x\geq 0}$.

In fact, we draw the graph of $(S^-)^{-1}$ and $S^+$ in a way that does not change the number of their intersections but is more intuitive. With the exception of a double fold singularity at $x = -y_t^- = -y_t^+$, it is not difficult to see that the number of intersections of $f^-$ and $f^+$ is equal to the number of crossing limit cycles of the system (9). We know that $f_2^-$ is increasing from *(b2)* in Theorem 3.1. In addition, if $\lambda_1^- + \lambda_2^- > 0$ and $\Delta_l(k^-) \triangleq K_l(t_l(k^-)) - k^- > 0$, function $f_2^-$ is first concave and then convex with the increase of $x_1^-$ from *(d2-B2)* in Theorem 3.1. Therefore, there exists $y^* < y_l$ (see Figure 10) to make the straight line connecting the points $(0, y^*)$ and $(x_u^-, y_s^-)$ tangent to the graph of the function $f_2^-$.

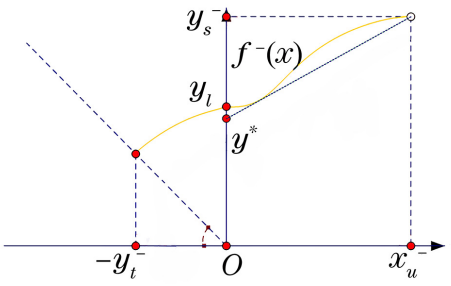


Figure 10: The sketch of $y^*$.

**Theorem 5.1.** Assume that $\lambda_1^- + \lambda_2^- > 0$, $k^- = \dfrac{\lambda_1^-\lambda_2^-}{1-\lambda_1^--\lambda_2^-} + 1$, $a < \lambda_1^+$, $k^+ = p(a)$ (see *(21)* for $p(a)$), and $\lambda_1^+ + \lambda_2^+ = 0$. For every $b_p \in (y^*, min\{y_s^-, 2y_t^-\})$, there exists $\delta(b_p) > 0$ such that for every $k_p \in (\dfrac{y_s^- - b_p}{x_u^-}, \dfrac{y_s^- - b_p}{x_u^-} + \delta(b_p))$, system *(11)* has 3 crossing limit cycles.

*Proof.* Our discussion is based on $f^-$ and $f^+$:

(I) We have the following results for $f^-$. $f_1^-, f_2^-$ are increasing by *(b1)* and *(b2)* in Theorem 3.1 respectively. If $\lambda_1^- + \lambda_2^- > 0$, from *(d1)* in Theorem 3.1, $f_1^-$ is convex. If $\lambda_1^- + \lambda_2^- > 0$ and $k^- = \frac{\lambda_1^-\lambda_2^-}{1-\lambda_1^--\lambda_2^-} + 1$. From *(d2-C)* in Theorem 3.1, $\Delta_l(k^-) > 0$. From *(d2-B2)* in Theorem 3.1, $f_2^-$ is first concave and then convex. From *(c2)* in Therem 3.1, slope of $f_2^-$ is equal to 0 at $x = 0$ and $x = x_u^-$;

(II) We have the following results for $f^+$. If $\lambda_1^+ + \lambda_2^+ = 0$, so from *(d1)* in Theorem 4.2 and Remark 4.2, the graph of $f_1^+$ is a straight line of slope 1. If $a < \lambda_1^+, k^+ = p(a)$, so from Case 3 in Theorem 4.6, the graph of $f_2^+$ is straight line of slope $k_p$ and $y_r = b_p$.

Noting that now if $x_e^+$ is fixed, right system in system (11) can be determined by $a$ and $\lambda_2^+$. Moreover, through Case 3 in Theorem 4.6 when $\lambda_1^+ + \lambda_2^+ = 0$, we get following relations

$$a = -(\frac{b_p}{2x_e^+} + k_p), \quad \lambda_2^+ = \sqrt{(\frac{b_p}{2x_e^+})^2 + \frac{k_p b_p}{x_e^+}}.$$

Therefore, $f^+$ can be determined by $k_p$ and $b_p$ instead of $a$ and $\lambda_2^+$ ($a < -\lambda_2^+$). We know $f_2^-, f_2^+$ have no intersections if $b_p \geq y_s^-$ because $k_p$ is positive. Here, we consider the case $b_p < y_s^-$. Therefore, we classify and discuss different results according to the range of $b_p$:

(1) if we set $b_p \in (y_l, y_s^-)$ and $k_p \in (\frac{y_s^- - b_p}{x_u^-}, \frac{y_s^- - b_p}{x_u^-} + \delta(b_p))$, then $f_2^-, f_2^+$ have 2 intersections. Specially, when $k_p = \frac{y_s^- - b_p}{x_u^-}$, the graph of $f_2^+$ passes through point $(x_u^-, y_s^-)$; when $k_p = \frac{y_s^- - b_p}{x_u^-} + \delta(b_p)$, the graph of $f_2^+$ is tangent to that of $f_2^-$;

(2) if we set $b_p \in (y^*, y_l]$ and $k_p \in (\frac{y_s^- - b_p}{x_u^-}, \frac{y_s^- - b_p}{x_u^-} + \delta(b_p))$, then $f_2^-, f_2^+$ have 3 intersections;

(3) if we set $b_p \in (y_l, 2y_t^-)$, then $f_1^-, f_1^+$ have 1 intersection;

(4) if we constrain $b_p \leq y_l$, then $f_1^-, f_1^+$ have no intersections.

In conclusion, when $b_p \in (y^*, min\{y_s^-, 2y_t^-\})$ and $k_p \in (\frac{y_s^- - b_p}{x_u^-}, \frac{y_s^- - b_p}{x_u^-} + \delta(b_p))$, $f^-$ and $f^+$ have 3 intersections. ■

Now let's consider other parameter conditions to get different results. Define follow equations about parameters $a, \lambda_1^+, \lambda_2^+, k^+, x_e^+$

$$b_p = \sigma_1, y_t^+ = \sigma_2, k_p = \sigma_3, \tag{26}$$

and a function

$$l(\lambda_2^+) = \lambda_2^+ \ln(1 + \frac{\frac{\sigma_1}{x_e^+}}{\lambda_2^+ - \frac{\sigma_1 - \sigma_2}{x_e^+}}) + (\frac{\frac{\sigma_3\sigma_1}{x_e^+}}{\lambda_2^+ - \frac{\sigma_1 - \sigma_2}{x_e^+}} - \frac{\sigma_1 - \sigma_2}{x_e^+}) \ln(1 - \frac{\lambda_2^+ - \frac{\sigma_1 - \sigma_2}{x_e^+}}{\sigma_3}), \tag{27}$$

where $\sigma_1, \sigma_2, \sigma_3$ are constants and $\sigma_1 > \sigma_2 > 0$, $\sigma_3 > 0$.

**Lemma 5.2.** Equation

$$l(\lambda_2^+) = 0 \tag{28}$$

has at least a solution for $\lambda_2^+ \in (\frac{\sigma_1 - \sigma_2}{x_e^+}, \frac{\sigma_1 - \sigma_2}{x_e^+} + \sigma_3)$.

*Proof.* $l(\lambda_2^+)$ is continuous in $(\frac{\sigma_1 - \sigma_2}{x_e^+}, \frac{\sigma_1 - \sigma_2}{x_e^+} + \sigma_3)$. Moreover, we have $\lim_{\lambda_2^+ \to \frac{\sigma_1 - \sigma_2}{x_e^+}} l(\lambda_2^+) = +\infty$ and $\lim_{\lambda_2^+ \to \frac{\sigma_1 - \sigma_2}{x_e^+} + \sigma_3} l(\lambda_2^+) = -\infty$, so Lemma 5.2 holds. ■

**Lemma 5.3.** Assume that $a < \lambda_1^+$ and $k^+ = p(a)$(*see (21) about* $k^+$ *and* $p(a)$). Solution of equations *(26)* can be expressed as

$$\begin{cases} \lambda_2^+ = s^*, \\ \lambda_1^+ = \dfrac{\sigma_1 - \sigma_2}{x_e^+} - \dfrac{\frac{\sigma_3\sigma_1}{x_e^+}}{s^* - \frac{\sigma_1 - \sigma_2}{x_e^+}}, \\ a = s^* - \dfrac{\sigma_3 \frac{\sigma_1}{x_e^+}}{s^* - \frac{\sigma_1 - \sigma_2}{x_e^+}} - \sigma_3, \end{cases} \tag{29}$$

where $s^*$ is the solution of equation *(27)* about $\lambda_2^+$ in $(\frac{\sigma_1 - \sigma_2}{x_e^+}, \frac{\sigma_1 - \sigma_2}{x_e^+} + \sigma_3)$.

*Proof.* Let $k^+ = p(a)$ and $x_e^+$ be fixed, then the equations (26) are now with respect to $a, \lambda_1^+, \lambda_2^+$. From (21), (22) and (23) we can get $b_p = x_e^+(\lambda_1^+ + \lambda_2^+ - 2a - k_p + p(a))$. Then the equations (26) can be expressed in the following form

$$\begin{cases} l(\lambda_2^+) = 0, \\ \lambda_1^+ = \dfrac{\sigma_1 - \sigma_2}{x_e^+} - \dfrac{\frac{\sigma_3\sigma_1}{x_e^+}}{\lambda_2^+ - \frac{\sigma_1 - \sigma_2}{x_e^+}}, \\ a = \lambda_1^+ + \lambda_2^+ - \dfrac{\sigma_1 - \sigma_2}{x_e^+} - \sigma_3. \end{cases} \tag{30}$$

But notice that $a < \lambda_1^+ < 0$, we get

$$\frac{\sigma_1 - \sigma_2}{x_e^+} < \lambda_2^+ < \frac{\sigma_1 - \sigma_2}{x_e^+} + \sigma_3,$$

and then Lemma 5.2 holds. Therefore, Lemma 5.3 is proved. ■

**Theorem 5.4.** Assume that $\lambda_1^- + \lambda_2^- > 0$, $k^- = \dfrac{\lambda_1^-\lambda_2^-}{1-\lambda_1^- - \lambda_2^-} + 1$, $a < \lambda_1^+$ and $k^+ = p(a)$ (see *(21)* for $p(a)$). Based on Lemma 5.3, if $\sigma_1 \in (max\{y^*, y_t^-\}, y_l)$, $\sigma_2 \in (y_t^-, \sigma_1)$, then there exists $\delta(\sigma_1) > 0$ such that for every $\sigma_3 \in (\dfrac{y_s^- - \sigma_1}{x_u^-}, \dfrac{y_s^- - \sigma_1}{x_u^-} + \delta(\sigma_1))$, system *(11)* has at least 4 crossing limit cycles.

*Proof.* Similar to proving Theorem 5.1, for $f^-$ we have $f_1^-, f_2^-$ are increasing, $f_1^-$ is convex, and $f_2^-$ is first concave then convex. The slope of $f_2^-$ is equal to 0 at $x = 0$ and $x = x_u^-$. In addition, for $f^+$ we have $f_1^+$ is increasing. The graph of $f_2^+$ is a straight line of slope $k_p$ and $y_r = b_p$ (from Case 3 in Theorem 4.6).

We set $\sigma_1 \in (max\{y^*, y_t^-\}, y_l)$, $\sigma_2 \in (y_t^-, \sigma_1)$ and $\sigma_3 \in (\frac{y_s^- - \sigma_1}{x_u^-}, \frac{y_s^- - \sigma_1}{x_u^-} + \delta(\sigma_1))$ (the $\delta(\cdot)$ is the same as that in proof of Theorem 5.1). According to equations (26) and Lemma 5.3, then we have $b_p \in (max\{y^*, y_t^-\}, y_l) \subseteq (y^*, y_l]$ and $k_p \in (\frac{y_s^- - b_p}{x_u^-}, \frac{y_s^- - b_p}{x_u^-} + \delta(b_p))$. Therefore $f_2^-, f_2^+$ have 3 intersections. In addition, we have $b_p \in (max\{y^*, y_t^-\}, y_l)$ and $y_t^+ \in (y_t^-, b_p)$. So $f_1^-(0) > f_1^+(0)$ and $f_1^-(-y_t^-) < f_1^+(-y_t^-)$, then $f_1^-$ and $f_1^+$ have at least 1 intersection. In conclusion $f^-, f^+$ have at least 4 intersections. ■

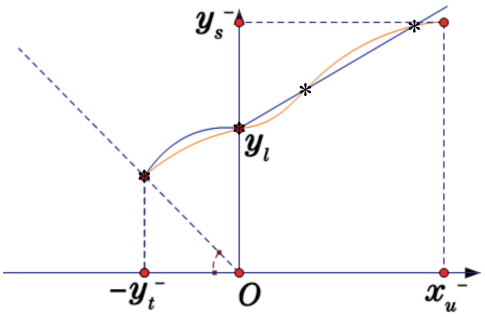


Figure 11: The sketch of 4 intersections "*" of $f^-$ (orange) and $f^+$ (blue).

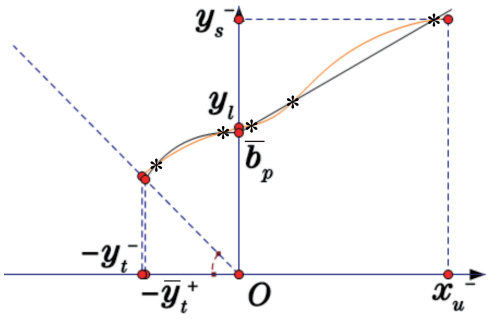


Figure 12: The sketch of 5 intersections "*" of $f^-$ (orange) and $\bar{f}^+$ (gray).

**Theorem 5.5.** Assume that $\lambda_1^- + \lambda_2^- > 0$, $k^- = \dfrac{\lambda_1^-\lambda_2^-}{1-\lambda_1^- - \lambda_2^-} + 1$, $a < \lambda_1^+$ and $k^+ = p(a)$ (see *(21)* for $p(a)$). We set $\sigma_1 = y_l, \sigma_2 = y_t^-$, then there exists $\delta(y_l) > 0$ such that for every $\sigma_3 \in (\dfrac{y_s^- - y_l}{x_u^-}, \dfrac{y_s^- - y_l}{x_u^-} + \delta(y_l))$, the conditions of Lemma 5.3 are met and system *(11)* has at least 3 limit cycles. Denoting $\bar{x}_e^+ = x_e^+ - \varepsilon$ and $\bar{\mathbf{x}}_e^+ = (\bar{x}_e^+, k^+\bar{x}_e^+)^T$. If

$$\frac{\lambda_1^- + \lambda_2^-}{\lambda_1^-\lambda_2^- x_e^-} > \frac{\lambda_1^+ + \lambda_2^+}{\lambda_1^+\lambda_2^+ x_e^+} > 0,$$

then for any sufficiently small $\varepsilon > 0$, the following system

$$\dot{\mathbf{x}} = \begin{cases} B^+(\mathbf{x} - \bar{\mathbf{x}}_e^+), & \mathbf{x} \in \Sigma_{\frac{\pi}{2}}^+, \\ B^-(\mathbf{x} - \mathbf{x}_e^-), & \mathbf{x} \in \Sigma_{\frac{\pi}{2}}^-. \end{cases} \tag{31}$$

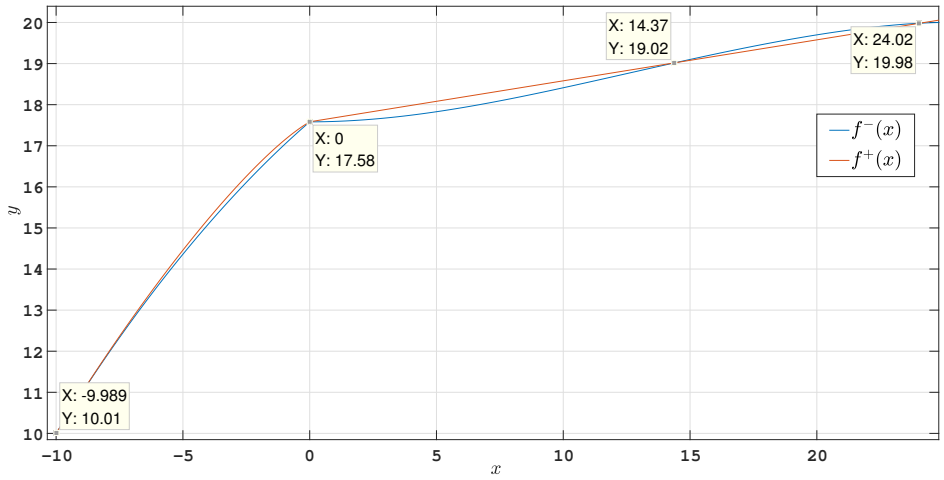


Figure 13: The graphs of $f^-$ and $f^+$ that possess 4 intersections.

has at least 5 limit cycles.

*Proof.* Similarly, we have $f_1^-, f_2^-$ are increasing, $f_1^-$ is convex, and $f_2^-$ is first concave then convex. The slope of $f_2^-$ is equal to 0 at $x = 0$ and $x = x_u^-$. For $f^+$ we have $f_1^+$ is increasing. The graph of $f_2^+$ is a straight line of slope $k_p$ and $y_r = b_p$.

We set $\sigma_1 = y_l, \sigma_2 = y_t^-$ and $\sigma_3 \in (\frac{y_s^- - y_l}{x_u^-}, \frac{y_s^- - y_l}{x_u^-} + \delta(y_l))$ (the $\delta(\cdot)$ is the same as that in proof of Theorem 5.1). According to equations (26) and Lemma 5.3, and then we have $b_p = y_l, y_t^+ = y_t^-$ and $k_p \in (\frac{y_s^- - y_l}{x_u^-}, \frac{y_s^- - y_l}{x_u^-} + \delta(y_l))$. Consequently, $f_1^-, f_1^+$ have at least 1 intersections of abscissas $y_t^-$ and $f_2^-, f_2^+$ have 3 intersections with an abscissa being 0 (see Figure 11). Since the intersection at $x = -y_t^-$ is not a limit cycle but a double fold singularity, system (11) has at least 3 limit cycles.

Next, to make $\frac{\mathrm{d}y_0^-}{\mathrm{d}y_1^-} > \frac{\mathrm{d}y_0^+}{\mathrm{d}y_1^+}$ at $-y_t^-$ so that $f_1^+$ ¿ $f_1^-$ in a small neighborhood of $-y_t^-$, we take Taylor expansions for $\frac{\mathrm{d}y_0^-(t)}{\mathrm{d}y_1^-(t)}$ and $\frac{\mathrm{d}y_0^+(t)}{\mathrm{d}y_1^+(t)}$ at $t = 0$ and get

$$\frac{\mathrm{d}y_0^\pm(t)}{\mathrm{d}y_1^\pm(t)} = -1 + \frac{2}{3}(\lambda_1^\pm + \lambda_2^\pm)t - \frac{2}{9}(\lambda_1^\pm + \lambda_2^\pm)^2 t^2 + o(t^2), \quad (t \to 0). \tag{32}$$

From the expressions of $y_1^\pm(t)$ and (19)), by the method of undetermined coefficients, we obtain the Taylor expansions

$$\begin{cases} y_1^-(t) = y_t^- - \lambda_1^-\lambda_2^- x_e^-(\frac{1}{2}t + \frac{\lambda_1^- + \lambda_2^-}{12}t^2 + o(t^2)), \quad (t \to 0) \\ t = -\frac{2}{\lambda_1^-\lambda_2^- x_e^-}(y_1^- - y_t^-) - \frac{2}{3}\frac{\lambda_1^- + \lambda_2^-}{(\lambda_1^-\lambda_2^- x_e^-)^2}(y_1^- - y_t^-)^2 + o((y_1^- - y_t^-)^2), \quad (y_1^- \to y_t^-) \\ y_1^+(t) = y_t^+ - \lambda_1^+\lambda_2^+ x_e^+(\frac{1}{2}t + \frac{\lambda_1^+ + \lambda_2^+}{12}t^2 + o(t^2)), \quad (t \to 0) \\ t = -\frac{2}{\lambda_1^+\lambda_2^+ x_e^+}(y_1^+ - y_t^+) - \frac{2}{3}\frac{\lambda_1^+ + \lambda_2^+}{(\lambda_1^+\lambda_2^+ x_e^+)^2}(y_1^+ - y_t^+)^2 + o((y_1^+ - y_t^+)^2), \quad (y_1^+ \to y_t^+) \end{cases} \tag{33}$$

Then by substituting the $t$ in (33) into (32), we get

$$\frac{\mathrm{d}y_0^{\pm}}{\mathrm{d}y_1^{\pm}} = -1 - \frac{4(\lambda_1^{\pm}+\lambda_2^{\pm})}{3\lambda_1^{\pm}\lambda_2^{\pm}x_e^{\pm}}(y_1^{\pm}-y_t^{\pm}) + o(y_1^{\pm}-y_t^{\pm}), \quad (y_1^{\pm}\to y_t^{\pm}).$$

If $\frac{\lambda_1^-+\lambda_2^-}{\lambda_1^-\lambda_2^-x_e^-} > \frac{\lambda_1^++\lambda_2^+}{\lambda_1^+\lambda_2^+x_e^+}$, then $\frac{\mathrm{d}y_0^-}{\mathrm{d}y_1^-} > \frac{\mathrm{d}y_0^+}{\mathrm{d}y_1^+}$ holds in a small neighborhood of $y_t^-$. Then $f_1^+$ will have values greater than $f_1^-$.

Noticing from (19) and (20) that the coordinates of the points on the graph of $f^+$ are all proportional to $x_e^+$, we appropriately reduce $x_e^+$ by a sufficiently small $\varepsilon$ ($\bar{x}_e^+ = x_e^+ - \varepsilon$) and keep other parameters unchanged, so that we get the system

$$\dot{\mathbf{x}} = B^+(\mathbf{x}-\bar{\mathbf{x}}_e^+), \quad \mathbf{x}\in\Sigma_{\frac{\pi}{2}}^+. \tag{34}$$

We denote $\bar{f}^+$ the function obtained in a similar way in Figure 9 of the system (34) and $\bar{f}_1^+ = \bar{f}^+|_{x<0}$, $\bar{f}_2^+ = \bar{f}^+|_{x\geq 0}$. Then $\bar{b}_p < b_p = y_l$, $\bar{y}_t^+ < y_t^+ = y_t^-$, where

$$\bar{b}_p = \bar{x}_e^+[(\lambda_2^+-a)^{\frac{-\lambda_1^+}{\lambda_2^+-\lambda_1^+}} - (\lambda_1^+-a)^{\frac{-\lambda_1^+}{\lambda_2^+-\lambda_1^+}}][(\lambda_2^+-a)^{\frac{\lambda_2^+}{\lambda_2^+-\lambda_1^+}} - (\lambda_1^+-a)^{\frac{\lambda_2^+}{\lambda_2^+-\lambda_1^+}}],\ \bar{y}_t^+ = -(a-k^+)\bar{x}_e^+,$$

but it still holds that $\bar{f}_1^+$ has values greater than $f_1^-$. Therefore, $\bar{f}_1^+$ has at least 2 intersections with $f_1^-$. $\bar{f}_2^+$ still has 3 intersections with $f_2^-$ for the continuity with respect to $x_e^+$ (see Figure 12). System (31) has at least 5 limit cycles. ■

Finally, we present a numerical example below obtained by Theorem 5.5. The parameters of the system (11) are

$$\lambda_1^- = -0.4,\ \lambda_2^- = 0.7,\ k^- = 0.6, \quad x_e^- = -25,\ x_e^+ = 1.2.$$

Then by setting $\sigma_1 = y_l = 17.5817$, $\sigma_2 = y_t^- = -10$, $\sigma_3 = 0.0997$, from (28) and $k^+ = p(a)$, we get

$$\lambda_1^+ = -8.7105,\ \lambda_2^+ = 6.4171,\ a = -8.7130,\ k^+ = -0.3794.$$

We can see (from Figure 13) $f^-$ and $f^+$ have 4 intersections. By letting $\varepsilon = 0.002$, $\bar{x}_e^+ = 1.198$. We denote the graph of the system $A^+(\mathbf{x}-\bar{\mathbf{x}}_e^+), \quad \mathbf{x}\in\Sigma_{\frac{\pi}{2}}^+$ obtained by the way in Figure 9 as $\bar{f}^+$. Then $f^-$ has 5 intersections with $\bar{f}^+$ (see Figure 14 and Figure 15). It is direct to verify that $\frac{\lambda_1^-+\lambda_2^-}{\lambda_1^-\lambda_2^-x_e^-} > \frac{\lambda_1^++\lambda_2^+}{\lambda_1^+\lambda_2^+x_e^+} > 0$ holds in this example. The ordinates of intersections are approximately $y_1 = 12.34, y_2 = 17.49, y_3 = 17.58, y_4 = 18.91, y_5 = 19.99$. So there are 2 limit cycles that only cross the positive $y$-axis and 3 limit cycles that cross both the positive $y$-axis and the positive $x$-axis. Furthermore, in this example $y_4, y_5 > y_u^+ = 17.67$. This means that there are 2 limit cycles to the right of $UM^+$ in the first quadrant. Therefore, we give the numerical phase portrait of the 5 limit cycles (see Figure 16).

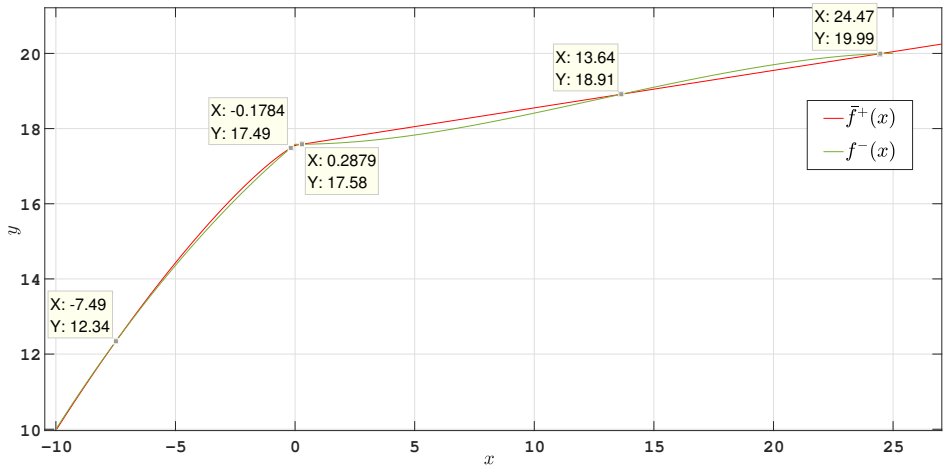


Figure 14: The graphs of $f^-$ and $\bar{f}^+$ that possess 5 intersections.

## 6. Proof of results about section maps $S^-$ and $S^+$

### *6.1. Proof of Theorem 3.1*

*Proof.* We substitute $\mathbf{\Phi}^-(t,(0,y_0^-)) = (0,y_1^-)$ and $\mathbf{\Phi}^-(t,(0,y_0^-)) = (x_1^-,0)$ into (13), then expressions (14) and (15) can be obtained excluding the range of $t$. By substituting $y_1^- \geq 0$ into (14), we obtain $h_l(t) \leq 0$, which is equivalent to $t \leq t_l$ (see Figure 15). Thus (14) is obtained. From (15) we know that $x_1^- > 0$ is equivalent to $h_l > 0$ ($t > t_l$) if $m_l > 0$ and to $h_l < 0$ ($t < t_l$) if $m_l < 0$ (recall that $m_l(t) = (1-\lambda_2^-)e^{\lambda_2^- t} - (1-\lambda_1^-)e^{\lambda_1^- t}$). We will try to figure out the sign of $m_l$ by figuring out the magnitude of $t_l$ and the $t$ in (15) later. *(a1)* and *(a2)* can be obtained directly from $h_l(t_l) = 0$, (14) and (15).

To examine the monotonicity and convexity, we take the derivative of (14) and (15) then get respectively

$$\frac{\mathrm{d}y_0^-(t)}{\mathrm{d}t} = \frac{\lambda_2^- e^{-\lambda_1^- t} - \lambda_1 e^{-\lambda_2^- t} - (\lambda_2^- - \lambda_1^-)}{(e^{\lambda_2^- t} - e^{\lambda_1^- t})^2} \cdot (\lambda_2^- - \lambda_1^-)e^{(\lambda_1^- + \lambda_2^-)t}(-x_e^-), \tag{35}$$

$$\frac{\mathrm{d}y_0^-(t)}{\mathrm{d}y_1^-(t)} = -\frac{\lambda_2^- e^{-\lambda_1^- t} - \lambda_1 e^{-\lambda_2^- t} - (\lambda_2^- - \lambda_1^-)}{\lambda_2^- e^{\lambda_1^- t} - \lambda_1 e^{\lambda_2^- t} - (\lambda_2^- - \lambda_1^-)}, \tag{36}$$

$$\frac{\mathrm{d}\frac{\mathrm{d}y_0^-(t)}{\mathrm{d}y_1^-(t)}}{\mathrm{d}t} = \frac{(\lambda_2^- - \lambda_1^-)[\cosh(\lambda_1^- t) - \cosh(\lambda_2^- t)] + (\lambda_1^- + \lambda_2^-)[\cosh((\lambda_2^- - \lambda_1^-)t) - 1]}{[\lambda_2^- e^{\lambda_1^- t} - \lambda_1 e^{\lambda_2^- t} - (\lambda_2^- - \lambda_1^-)]^2/(-2\lambda_1^-\lambda_2^-)}, \tag{37}$$

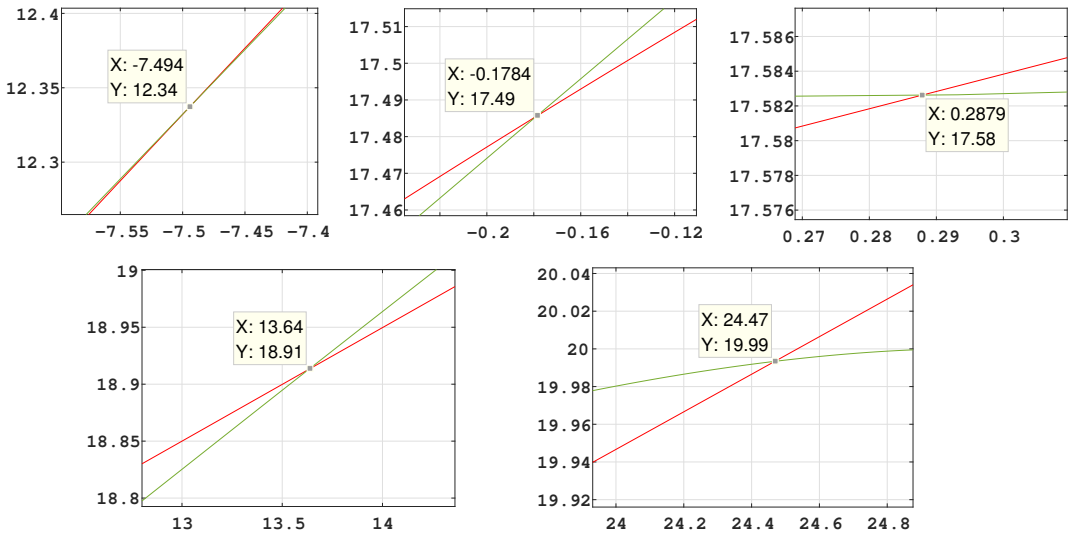


Figure 15: The details of the graphs.

and

$$\frac{\mathrm{d}y_0^-(t)}{\mathrm{d}t} = \frac{g_l(t)}{m_l^2(t)} \cdot (\lambda_2^- - \lambda_1^-)e^{(\lambda_1^- + \lambda_2^-)t}(-x_e^-), \tag{38}$$

$$\frac{\mathrm{d}y_0^-(t)}{\mathrm{d}x_1^-(t)} = \frac{g_l(t)}{\lambda_2^-(1-\lambda_1^-)e^{\lambda_1^- t} - \lambda_1^-(1-\lambda_2^-)e^{\lambda_2^- t} - (\lambda_2^- - \lambda_1^-)k^-}, \tag{39}$$

$$\frac{\mathrm{d}\frac{\mathrm{d}y_0^-(t)}{\mathrm{d}x_1^-(t)}}{\mathrm{d}t} = -\frac{D_l(t;k^-)\cdot m_l(t)(-\lambda_1^-\lambda_2^-)e^{-(\lambda_1^- + \lambda_2^-)t}}{[\lambda_2^-(1-\lambda_1^-)e^{\lambda_1^- t} - \lambda_1^-(1-\lambda_2^-)e^{\lambda_2^- t} - (\lambda_2^- - \lambda_1^-)k^-]^2}, \tag{40}$$

where $g_l(t) = [\lambda_2^-(1-\lambda_2^-)e^{-\lambda_1^- t} - \lambda_1(1-\lambda_1^-)e^{-\lambda_2^- t}]k^- - (\lambda_2^- - \lambda_1^-)(1-\lambda_1^-)(1-\lambda_2^-)$,
$D_l(t;k^-) = (\lambda_2^- - \lambda_1^-)k^{-2} + (\lambda_1^- + \lambda_2^-)m_l(t)k^- - (\lambda_2^- - \lambda_1^-)(1-\lambda_1^-)(1-\lambda_2^-)e^{(\lambda_1^- + \lambda_2^-)t}$.

For *(b1)* and *(b2)*, noticing through qualitative analysis that $\frac{\mathrm{d}y_0^-}{\mathrm{d}y_1^-} \leq 0$ and $\frac{\mathrm{d}y_0^-}{\mathrm{d}x_1^-} \geq 0$, we only need to determine the sign of (35) and (38) then the sign of $\frac{\mathrm{d}y_1^-(t)}{\mathrm{d}t}$ and $\frac{\mathrm{d}x_1^-(t)}{\mathrm{d}t}$ can be determined. It is direct to verify that (35) is positive. For (38), we denote the zero point of $g_l(t)$ as $t_{g_l}^0$. By substituting $g_l(t_{g_l}^0) = 0$ in to $h_l(t_{g_l}^0)$, we can get

$$h_l(t_{g_l}^0) = \frac{[(1-\lambda_1^-)(1-\lambda_2^-) - k^-(1-\lambda_1^- - \lambda_2^-)](\lambda_2^- - \lambda_1^-)}{\lambda_2^-(1-\lambda_2^-)k^-}(k^- e^{-\lambda_2^- t_{g_l}^0} - (1-\lambda_2^-))$$
$$\begin{cases} \sim k^- e^{-\lambda_2^- t_{g_l}^0} - (1-\lambda_2^-), & \text{if } k^- \neq \frac{\lambda_1^-\lambda_2^-}{1-\lambda_1^--\lambda_2^-} + 1, \\ = 0, & \text{if } k^- = \frac{\lambda_1^-\lambda_2^-}{1-\lambda_1^--\lambda_2^-} + 1, \end{cases}$$

where we use "$\sim$" to mean that they have the same sign. Then we denote $F(t) = k^- e^{-\lambda_2^- t} -$

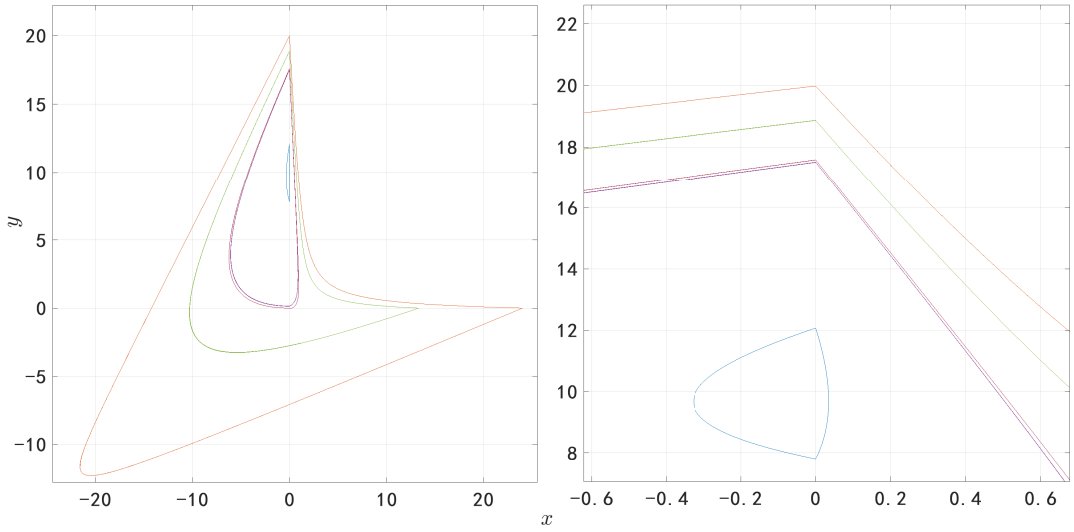


Figure 16: The phase portrait of 5 limit cycles.

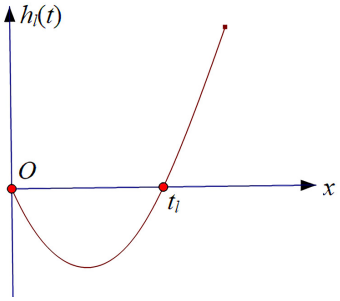


Figure 17: The graph sketch of $h_l(t)$.

$(1-\lambda_2^-)$, and the zero point of it as $t_F^0$. By substituting $t_F^0$ into $g_r(t)$ we get

$$g_l(t_F^0) = \lambda_2^-(1-\lambda_2^-)[k^- e^{-\lambda_1^- t_F^0} - (1-\lambda_1^-)] \sim k^- - [\frac{(1-\lambda_1^-)^{\lambda_2^-}}{(1-\lambda_2^-)^{\lambda_1^-}}]^{\frac{1}{\lambda_2^- - \lambda_1^-}}.$$

Using numerical methods, we can verify that $\frac{\lambda_1^-\lambda_2^-}{1-\lambda_1^--\lambda_2^-} + 1 < [\frac{(1-\lambda_1^-)^{\lambda_2^-}}{(1-\lambda_2^-)^{\lambda_1^-}}]^{\frac{1}{\lambda_2^- - \lambda_1^-}}$ $(0 < \lambda_2 < 1)$, which means $g_l(t_F^0) < 0$ and $t_F^0 < t_{g_l}^0$. Subsequently $F(t_{g_l}^0) < 0$ which means $h_l(t_{g_l}^0) \leq 0$ and $t_{g_l}^0 \leq t_l$. Note that the $t$ in (15) can reach $+\infty$, so $g_l(t) > 0$ for all $t > t_l$. Consequently (38) is positive, then $\frac{\mathrm{d}x_1^-(t)}{\mathrm{d}t}$ is always positive when $t \in (t_l, +\infty)$. Therefore $x_1^- > 0$ is equivalent to $t > t_l$, and $m_l > 0$ when $t > t_l$. In conclusion $t \in (t_l, +\infty)$ in (15). *(c1)* and *(c2)* can be deduced direcly from (36) and (39).

As for *(d1)*, we expand the molecule in (37) into the Taylor series

$$\begin{aligned}&(\lambda_2^- - \lambda_1^-)[\cosh(\lambda_1^- t) - \cosh(\lambda_2^- t)] + (\lambda_1^- + \lambda_2^-)[\cosh((\lambda_2^- - \lambda_1^-)t) - 1]\\ &= (\lambda_2^- - \lambda_1^-)(\lambda_1^- + \lambda_2^-)\sum_{n=1}^{\infty}\sum_{i=0}^{2n-1}[(C_{2n-1}^i - 1)(\lambda_2^-)^{2n-1-i}(-\lambda_1^-)^i]\\ &\sim \lambda_1^- + \lambda_2^-,\end{aligned}$$

then by verifying the sign of (37), *(d1)* can ba obtained.

For *(d2-A)*, we take the derivation of $D_l(t;k^-)$ in (40) and get

$$\frac{\mathrm{d}D_l}{\mathrm{d}t} = (\lambda_1^- + \lambda_2^-)e^{(\lambda_1^- + \lambda_2^-)t}g_l(t).$$

When $\lambda_1^- + \lambda_2^- \le 0$, $\frac{\mathrm{d}D_l}{\mathrm{d}t} \le 0$. Noting that $D_l(0;k^-) < 0$, we have $D_l < 0$. Thus because $D_l(t;k^-) \sim -\frac{\mathrm{d}^2 y_0^-}{\mathrm{d}x_1^{-2}}$, $\frac{\mathrm{d}^2 y_0^-}{\mathrm{d}x_1^{-2}} > 0$.

For *(d2-B)*, when $\lambda_1^- + \lambda_2^- > 0$, through the root formula we write $D(t;k^-)$ as

$$D_l(t;k^-) = (k - K_l(t))(k - K_l'(t))$$

where

$$K_l'(t) = \frac{-(\lambda_1^- + \lambda_2^-)m_l(t) - \sqrt{(\lambda_1^- + \lambda_2^-)^2 m_l^2(t) + 4(\lambda_2^- - \lambda_1^-)^2(1-\lambda_1^-)(1-\lambda_2^-)e^{(\lambda_1^- + \lambda_2^-)t}}}{2(\lambda_2^- - \lambda_1^-)}.$$

It is not difficult to see that $K_l > 0$ and $K_l' < 0$, so in order to determine the sign of $D_l(t;k^-)$ we only need to consider whether it is possible that $K_l(t) = k^-$. Noting that $\frac{\mathrm{d}D_l}{\mathrm{d}t} > 0$, we have $\forall t_1 < t_2$, $0 = (K_l(t_1) - K_l(t_1))(K_l(t_1) - K_l'(t_1)) < (K_l(t_1) - K_l(t_2))(K_l(t_1) - K_l'(t_2))$. So $K_l(t)$ is decreasing and $K_l(t) \in (0, K_l(t_l))$. Now we need to determine the sign of $K_l(t_l) - k^-$. (17) can be obtained from $h_l(t_l) = 0$. And by direct calculation we can get $\frac{\mathrm{d}k^-}{\mathrm{d}t_l} < 0$, so the inverse function $t_l(k^-)$ exists. Then *(d2-B)* can be obtained.

As for *(d2-C)*, we have to remind that when $k^- \to 1 - \lambda_2^-$, $t_l \to +\infty$, which can be obtained from $h_l(t_l) = 0$. In addition, from (16) we have $\lim_{t\to+\infty} K_l(t) = 0$. So when $k^- \to 1 - \lambda_2^-$, $\Delta_l(k^-) = K_l(t_l) - k^- < 0$. When $k^- = \frac{\lambda_1^-\lambda_2^-}{1-\lambda_1^--\lambda_2^-} + 1$, noting that $\frac{\mathrm{d}y_0^-}{\mathrm{d}x_1^-}|_{x_1^-\to 0} = 0$ and $\lim_{x_1^-\to x_u^-}\frac{\mathrm{d}y_0^-}{\mathrm{d}x_1^-} = 0$, it is not hard to obtain that $\exists\xi \in (0, x_u^-)$ s.t. $\frac{\mathrm{d}^2 y_0^-}{\mathrm{d}x_1^{-2}}|_{x_1^-=\xi} = 0$ by differential mean value theorem and intermediate value theorem. ■

### 6.2. *Proof of Theorem 4.2-4.6*

Because the proof method is basically the same as that in proving Theorem 3.1, we will only give some of the more important details of $S_2^+$ and do not talk about $S_1^+$.

*Proof.* We will first figure out the sign of $m_r(t)$ and $g_r(t)$ which plays the key role in determining $S_2^+$ and in dividing it into five categories to discuss.

It is not difficult to verify by direct calculation that $m_r(0) = \lambda_2^+ - \lambda_1^+ > 0$, $g_r(0) = [(a-\lambda_1^+-\lambda_2^+)k^+ - (a-\lambda_1^+)(a-\lambda_2^+)] \geq 0$. When $k^+ > 0$ or $k^+ = 0$ or $a = \lambda_1^+$, $g_r(t) > 0$. When $a \geq \lambda_1^+$,$m_r(t) > 0$. From (20) we have

$$\frac{\mathrm{d}y_0^+(t)}{\mathrm{d}t} = \frac{g_r(t)}{m_r^2(t)} \cdot (\lambda_2^+ - \lambda_1^+)e^{-(\lambda_1^+ + \lambda_2^+)t}x_e^+,$$

where $t \in (t_r, +\infty)$ in Theorem 4.2, 4.3 and 4.5. However the sign of $m_r(t)$ when $a < \lambda_1^+$ and the sign of $g_r(t)$ when $k < 0, a > \lambda_1^+$ or $a < \lambda_1^+$ are not apparent. So we denote the zero point of $g_r(t)$ as $t_{g_r}^0$, and substitute it into $h_r(t)$,

$$h_r(t_{g_r}^0) = [k^+e^{\lambda_2^+ t_{g_r}^0} - (a-\lambda_2^+)]\frac{(\lambda_2^+ - \lambda_1^+)[(a-\lambda_1^+)(a-\lambda_2^+) - (a-\lambda_1^+-\lambda_2^+)k^+]}{\lambda_2^+ k^+(a-\lambda_2^+)}$$
$$\begin{cases} \sim -[k^+e^{\lambda_2^+ t_{g_r}^0} - (a-\lambda_2^+)], & \text{if } k \neq \frac{\lambda_1^+\lambda_2^+}{a-\lambda_1^+-\lambda_2^+} + a, \\ = 0, \quad \text{if } k = \frac{\lambda_1^+\lambda_2^+}{a-\lambda_1^+-\lambda_2^+} + a. \end{cases}$$

Then we denote $G(t) = k^+e^{\lambda_2^+ t_{g_r}^0} - (a-\lambda_2^+)$ and the zero point of it as $t_G^0$. By substituting $t_G^0$ into $g_r(t)$ we get

$$g_r(t_G^0) = \lambda_2^+(a-\lambda_2^+)[k^+e^{\lambda_1^+ t_G^0} - (a-\lambda_1^+)] \begin{cases} > 0, \text{ if } k < 0, a > \lambda_1^+, \\ \sim p(a) - k^+, \text{ if } a < \lambda_1^+. \end{cases}$$

We can verify through numerical method that $a < p(a) \leq \frac{\lambda_1^+\lambda_2^+}{a-\lambda_1^+-\lambda_2^+} + a$ when $a \leq \lambda_1^+$, where the equal sign is only taken when $a = \lambda_1^+$. So we have

$$t_r > t_{g_r}^0 \text{ when } k < 0, a > \lambda_1^+ \text{ or } a < \lambda_1^+, a < k < p(a);$$
$$t_r < t_{g_r}^0 \text{ when } a < \lambda_1^+, p(a) < k < \frac{\lambda_1^+\lambda_2^+}{a-\lambda_1^+-\lambda_2^+} + a;$$
$$t_r = t_{g_r}^0 \text{ when } a < \lambda_1^+, k = p(a) \text{ or } a < \lambda_1^+, k = \frac{\lambda_1^+\lambda_2^+}{a-\lambda_1^+-\lambda_2^+} + a.$$

When $k < 0, a > \lambda_1^+$, $g_r(t_r) > 0$. $x_1^+$ increases as $t$ increases from $t_r$ until $t$ reaches $t_{g_r}^0$, where we can find that it is the time corresponding to the trajectory tangent to the $x$-axis. So in this case (Theorem 4.4) $t \in (t_r, t_{g_r}^0]$.

When $a < \lambda_1^+$, we denote the zero point of $m_r(t)$ as $t_{m_r}^0$ and substitute it into $h_r(t)$.

$$h_r(t_{m_r}^0) = \frac{(\lambda_2^+ - \lambda_1^+)[k^+e^{\lambda_2^+ t_{m_r}^0} - (a-\lambda_2^+)]}{a-\lambda_2^+} \sim -G(t_{m_r}^0).$$

Then we substitute $t_G^0$ into $m_r(t)$ and get

$$m_r(t_G^0) \sim g_r(t_G^0),$$

which means that

$$
\begin{aligned}
&t_r < t^0_{m_r} \text{ when } a < \lambda_1^+, a < k < p(a);\\
&t_r > t^0_{m_r} \text{ when } a < \lambda_1^+, p(a) < k \le \frac{\lambda_1^+\lambda_2^+}{a-\lambda_1^+-\lambda_2^+} + a;\\
&t_r = t^0_{m_r} \text{ when } a < \lambda_1^+, k = p(a).
\end{aligned}
$$

So now it is not hard to obtain that $t \in (t_r, t^0_{m_r})$ when $a < \lambda_1^+, a < k < p(a)$, and $t \in (t^0_{m_r}, t_r)$ when $a < \lambda_1^+, p(a) < k \le \frac{\lambda_1^+\lambda_2^+}{a-\lambda_1^+-\lambda_2^+} + a$. In addition, from $h_r(t_r) = 0$ we can verify that $t_r \to t^0_{m_r}$ when $k^+ \to p(a)$, so $t$ is always equal to $t^0_{m_r}$ when $k^+ = p(a)$. These form the three cases in Theorem 4.6.

Next we prove some results in Case 1 of Theorem 4.6. *(a1)*, *(b1)*, *(d1-A)*, *(d1-B)* can be deduced similar to proof of Theorem 3.1.

To obtain *(c1)*, remind that $k_p = \lim\limits_{t\to t^0_{m_r}} \dfrac{y_0^+(t)}{x_1^+(t)}$ and $b_p = \lim\limits_{t\to t^0_{m_r}} y_0^+(t) - k_p x_1^+(t)$.

For *(d1-C)*, similarly we get by seeking derivation that

$$
\begin{aligned}
\frac{\mathrm{d}\frac{\mathrm{d}y_0^+(t)}{x_1^+(t)}}{\mathrm{d}t} &= -\frac{D_r(t;k^+)\cdot m_r(t)(-\lambda_1^+\lambda_2^+)e^{(\lambda_1^+ + \lambda_2^+)t}}{[\lambda_2^+(a-\lambda_1^+)e^{-\lambda_1^+ t} - \lambda_1^+(a-\lambda_2^+)e^{-\lambda_2^+ t} - k(\lambda_2^+ - \lambda_1^+)]^2},\\
\frac{\mathrm{d}x_1^+(t)}{\mathrm{d}t} &= \frac{g_r(t)}{m_r^2(t)}\cdot(\lambda_2^+ - \lambda_1^+)e^{-(\lambda_1^+ + \lambda_2^+)t}x_e^+,
\end{aligned}
$$

where $D_r(t;k^+) = (\lambda_2^+ - \lambda_1^+){k^+}^2 - (\lambda_1^+ + \lambda_2^+)m_r(t)k^+ - (\lambda_2^+ - \lambda_1^+)(a-\lambda_1^+)(a-\lambda_2^+)e^{-(\lambda_1^+ + \lambda_2^+)t}$. From these relations we can know that

$$
D_r(t;k^+) \sim -\frac{\mathrm{d}^2 y_0^+}{\mathrm{d}{x_1^+}^2}.
$$

Then we have from (25)

$$
\frac{\mathrm{d}k^+}{\mathrm{d}t_r} = \frac{\lambda_2^+ e^{-\lambda_1^+ t_r} - \lambda_1^+ e^{-\lambda_2^+ t_r} - (\lambda_2^+ - \lambda_1^+)}{(e^{\lambda_2^+ t_r} - e^{\lambda_1^+ t_r})^2}\cdot(\lambda_2^+ - \lambda_1^+)e^{(\lambda_1^+ + \lambda_2^+)t_r},
$$

and

$$
\frac{\mathrm{d}t_r}{\mathrm{d}k^+}|_{k^+ = p(a)} = \frac{1}{(q(a)-p(a))(\lambda_1^+ + \lambda_2^+ - a)} \triangleq l > 0,
$$

where $q(a) = \frac{\lambda_1^+\lambda_2^+}{a-\lambda_1^+-\lambda_2^+} + a$. Now we make Taylor expansion

$$
\begin{aligned}
&t_r = t^0_{m_r} + l(k^+ - p(a)) + o(k^+ - p(a)), \quad (k^+ \to p(a))\\
&e^{\sigma(t_r - t^0_{m_r})} = 1 + \sigma l(k - p(a)) + o(k^+ - p(a)), \quad (k^+ \to p(a)).
\end{aligned}
$$

where $\sigma$ is an arbitrary constant, and get

$$D_r(t_r; k^+) = 2(\lambda_2^+ - \lambda_1^+)p(a)(k^+ - p(a)) + o(k^+ - p(a)), \quad (k^+ \to p(a)).$$

In addtion, by substituting $t_{m_r}^0$ into $D_r(t; k^+)$ we have

$$D_r(t_{m_r}^0; k^+) = (\lambda_2^+ - \lambda_1^+)(k^+ + p(a))(k^+ - p(a)),$$

from which we can obtain that $D_r(t_{m_r}^0; k^+) \sim D_r(t_r; k^+),\ (k^+ \to p(a))$. So there cannot exist a time $t_0$ such that $D_r(t_0; k^+)$ is opposite to $D_r(t_{m_r}^0; k^+)$ and $D_r(t_r; k^+)$ when $k^+ \to p(a)$, or there will be two inflection points.

Case 2 and Case 3 of Theorem 4.6 can be deduced similarly. ■

## 7. Summary

In our investigation, for a linear lateral system of S-S type, we simplified the system (reduced 3 parameters) by topological transformation under certain conditions, discussed the characteristics of the section maps, and obtained the conclusion that the system can have at least 5 limit cycles. In fact, we found a procedure that can be used to make such systems generate 3, 4 or 5 limit cycles in some cases. Some results about the number of limit cycles were obtained in the linear lateral system of F-F type. However, it is worth noting that in PWLS with a straight separation line, the F-F type systems can have more limit cycles than those of the S-S type. In this sense, our results are significant because it means that there are more limit cycles undiscovered in the F-F type lateral systems.

### Data Availability Statements

Data sharing is not applicable to this article as no new data were created or analyzed in this study.

### Conflict of interest

All co-authors have no conflict of interest to declare.


### Acknowledgments

This work was supported by the National Natural Science Foundation of China (NNSFC) (Nos. 12172340 and 12411530068), Shenzhen Science and Technology Program (No. JCYJ20240813114012016), High-level Talent Introduction Plan of Guangzhou City, the Fundamental Research Funds for the Central Universities-China University of Geosciences (Wuhan) (No. G1323524005), and the Young Top-notch Talent Cultivation Program of Hubei Province.

## References


[1] Andronov, A. A., Vitt, A. & Khaikin, S. [1966] *Theory of Osscillators*, (Pergamon Press, Oxford-NY-Toronto, Ont.).

[2] Artés, J. C., Llibre, J., Medrado, J. C. & Teixeira, M. A. [2014] "Piecewise linear differential systems with two real saddles," *Mathematics and Computers in Simulation* **95**, 13–22.

[3] Baymout, L., Benterki, B., & Llibre L. [2024] "Limit cycles of the discontinuous piecewise differential systems separated by a nonregular line and formed by a linear centerand a quadratic one," *International Journal of Bifurcation and Chaos* **34**, 2450058.

[4] Bernardo, M., Budd, C., Champneys, A. R. & Kowalczyk, P. [2008] *Piecewise-smooth dynamical systems: theory and applications*, (Springer Science & Business Media).

[5] Castillo, J., Llibre, J. & Verduzco, F. [2017] "The pseudo-Hopf bifurcation for planar discontinuous piecewise linear differential systems," *Nonlinear Dynamics* **90**, 1829–1840.

[6] Carmona, V., Freire, E., Ponce, E., Ros, J. & Torres, F. [2005] "Limit cycle bifurcation in 3d continuous piecewise linear systems with two zones: Application to chua's circuit," *International Journal of Bifurcation and Chaos* **15**, 3153–3164.

[7] Carmona, V., Fernández-Sánchez, F., Novaes, D. D. [2023] "Uniform upper bound for the number of limit cycles of planar piecewise linear differential systems with two zones separated by a straight line," *Applied Mathematics Letters* **137**, 108501.

[8] Cardin, P. T. & Torregrosa. J. [2016] "Limit cycles in planar piecewise linear differential systems with nonregular separation line," *Physica D: Nonlinear Phenomena* **337**, 67–82.

[9] Chen, H., Duan, S., Tang, Y. & Xie, J. [2018] "Global dynamics of a mechanical system with dry friction," *Journal of Differential Equations* **265**, 5490–5519.

[10] Chen, T., Huang, L. & Llibre, J. [2023] "Nonexistence and uniqueness of limit cycles in a class of three-dimensional piecewise linear differential systems," *International Journal of Bifurcation and Chaos* **33**, 2350075.

[11] Cristiano, R., Durval, J. T. & Mariana, Q. V. [2021] "Hopf-like bifurcations and asymptotic stability in a class of 3D piecewise linear systems with applications," *Journal of Nonlinear Science* **31**, 31–65.

[12] Dercole, F., Gragnani, A. & Rinaldi, S. [2007] "Bifurcation analysis of piecewise smooth ecological models," *Theoretical Population Biology* **72**, 197–213.

[13] Esteban, M., Llibre, J. & Valls. C. [2021] "The extended 16th Hilbert problem for discontinuous piecewise linear centers separated by a nonregular line," *International Journal of Bifurcation and Chaos* **31**, 2150225.

[14] Freire, E., Ponce, E., Rodrigo, F. & Torres. F. [1998] "Bifurcation sets of continuous piecewise linear systems with two zones," *International Journal of Bifurcation and Chaos* **8**, 2073–2097.

[15] Freire, E., Ponce, E. & Torres, F. [2015] "On the critical crossing cycle bifurcation in planar Filippov systems," *Journal of Differential Equations* **259**, 7086–7107.

[16] Freire, E., Ponce, E. & Torres. F. [2014] "A general mechanism to generate three limit cycles in planar Filippov systems with two zones," *Nonlinear Dynamics* **78**, 251–263.

[17] Freire, E., Ponce, E., Torregrosa, J., et al. [2021] "Limit cycles from a monodromic infinity in planar piecewise linear systems," *Journal of Mathematical Analysis and Applications* **496**(2), 124818.

[18] Glendinning, P. [2018] "Shilnikov chaos, Filippov sliding and boundary equilibrium bifurcations," *European Journal of Applied Mathematics* **29**, 757–777.

[19] Glendinning, P. & Jeffrey, M. R. [2019] *An introduction to piecewise smooth dynamics*, (World Scientific).

[20] Guardia, M., Seara, T. M. & Teixeira, M. A. [2011] "Generic bifurcations of low codimension of planar Filippov systems," *Journal of Differential Equations* **250**, 1967–2023.

[21] Henao, M. M., Cristiano, R., Pagano, D. J., Freire, E. & Ponce, E. [2022] "Bifurcation analysis of 3D-PWS systems with two transversal switching boundaries: A case study in power electronics," *Physica D* **442**, 133505.

[22] Hogan, S. J., Homer, M. E., Jeffrey, M. R. & Szalai, R. [2016] "Piecewise smooth dynamical systems theory: the case of the missing boundary equilibrium bifurcations," *Journal of Nonlinear Science* **26**, 1161–1173.

[23] Huan, S. M. & Yang, X. S. [2012] "On the number of limit cycles in general planar piecewise linear systems," *Discrete and Continuous Dynamical Systems* **32**(6), 2147–2164.

[24] Huan, S. & Yang. X. [2014] "On the number of limit cycles in general planar piecewise linear systems of node–node types," *Journal of Mathematical Analysis and Applications* **411**, 340–353.

[25] Huan, S. & Yang. X. [2019] "Limit cycles in a family of planar piecewise linear differential systems with a nonregular separation line," *International Journal of Bifurcation and Chaos* **29**, 1950109.

[26] Huang, L., & Wang, J. [2024] "Global dynamics of piecewise smooth systems with switches depending on both discrete times and status," *SIAM Journal on Applied Dynamical Systems* **23**, 2533-2556.

[27] Kuznetsov, Y. A., Rinaldi, S. & Gragnani, A. [2003] "One-parameter bifurcations in planar Filippov systems," *International Journal of Bifurcation and Chaos* **13**, 2157–2188.

[28] Li, T. & Chen, X. [2020] "Degenerate grazing-sliding bifurcations in planar Filippov systems," *Journal of Differential Equations* **269**, 11396–11434.

[29] Li, W., Huang, L. & Wang, J. [2021] "Global asymptotical stability and sliding bifurcation analysis of a general Filippov-type predator-prey model with a refuge," *Applied Mathematics and Computation* **405**, 126263.

[30] Li, Y., Wei, Z., Zhang, W. & Kapitaniak, T. [2023] "Melnikov-type method for chaos in a class of hybrid piecewise-smooth systems with impact and noise excitation under unilateral rigid constraint," *Applied Mathematical Modelling* **122**, 506–523.

[31] Liu, H., Wei, Z. & Moroz, I. [2023] "Limit cycles and bifurcations in a class of planar piecewise linear systems with a nonregular separation line," *Journal of Mathematical Analysis and Applications* **526**, 127318.

[32] Llibre, J. & Ponce, E. [2012] "Three nested limit cycles in discontinuous piecewise linear differential systems with two zones," *Dyn. Contin. Discrete Impuls. Syst. Ser. B Appl. Algorithms* **19**(3), 325–335.

[33] Llibre, J., Teixeira, M. A. & Torregrosa. J. [2013] "Lower bounds for the maximum number of limit cycles of discontinuous piecewise linear differential systems with a straight line of separation," *International Journal of Bifurcation and Chaos* **23**, 1350066.

[34] Llibre, J., Ponce, E. & Valls, C. [2019] "Two limit cycles in Liénard piecewise linear differential systems," *Journal of Nonlinear Science* **29**, 1499–1522.

[35] Lu, K., Yang, Q. & Xu, W. [2019] "Heteroclinic cycles and chaos in a class of 3D three-zone piecewise affine systems," *Journal of Mathematical Analysis and Applications* **478**, 58–81.

[36] Lum, R. & Chua. L. O. [1991] "Global properties of continuous piecewise linear vector fields. part I: Simplest case in $\mathbb{R}^2$," *International Journal of circuit theory and applications* **19**, 251–307.

[37] Novaes, D. D., Teixeira, M. A. & Zeli, I. O. [2018] "The generic unfolding of a codimension-two connection to a two-fold singularity of planar Filippov systems," *Nonlinearity* **31**, 2083–2104.

[38] Simpson, D. J. W. [2019] "Hopf-like boundary equilibrium bifurcations involving two foci in Filippov systems," *Journal of Differential Equations* **267**, 6133–6151.

[39] Simpson, D. J. W. [2010] *Bifurcations in piecewise-smooth continuous systems*, (World Scientific).

[40] Simpson, D. J. W. [2022] "Twenty Hopf-like bifurcations in piecewise-smooth dynamical systems," *Physics Reports* **970**, 1–80.

[41] Sun, L., & Du, Z. [2024] "Crossing limit cycles in planar piecewise linear systems separated by a nonregular line with node-node type critical point," *Journal of Nonlinear Science* **34**, 2450049.

[42] Wei, Z., Zhu, B. & Escalante-González, R. J. [2021] "Existence of periodic orbits and chaos in a class of three-dimensional piecewise linear systems with two virtual stable node-foci," *Nonlinear Analysis: Hybrid Systems* **43**, 101114.

[43] Wei, Z., & Wang, F. [2024] " Two-parameter bifurcations and hidden attractors in a class of 3D linear Filippov systems," *International Journal of Bifurcation and Chaos* **34**, 2450052.

[44] Wu, F., Huang, L. & Wang. J. [2021] "Sliding bifurcation in planar piecewise smooth systems with two Zones separated by an ellipse," *International Journal of Bifurcation and Chaos* **31**, 2150231.

[45] Zhao, Q., Wang, C. & Yu. J. [2021] "Limit cycles in discontinuous planar piecewise linear systems separated by a nonregular line of center–center type," *International Journal of Bifurcation and Chaos* **31**, 2150136.

[46] Zhao, Q. & Yu. J. [2019a] "Limit cycles of piecewise linear dynamical systems with three zones and lateral systems," *Journal of Applied Analysis and Computation* **9**, 1822–1837.

[47] Zhao, Q. & Yu. J. [2019b] "Poincaré maps of "¡"-shape planar piecewise linear dynamical systems with a saddle," *International Journal of Bifurcation and Chaos* **29**, 1950165.